A New Member of the 4-Methylideneimidazole-5-one-containing Aminomutase Family from the Enediyne Kedarcidin Biosynthetic Pathway

Sheng-Xiong Huang[a,1], Jeremy R. Lohman[a,1], Tingting Huang[a], and Ben Shen[a,b,c,2]

[a]Department of Chemistry, [b]Department of Molecular Therapeutics, and [c]Natural Products Library Initiative at The Scripps Research Institute, The Scripps Research Institute, Jupiter, Florida 33458, United States

[1]These authors contributed equally

[2]To whom correspondence should be addressed at: The Scripps Research Institute, 130 Scripps Way, #3A1, Jupiter, FL 33458. Email: shenb@scripps.edu

Supporting Online Materials

General experimental procedures

General instrumentation: PCR was performed with a BIO-RAD S1000™ Thermal cycler. ^{1}H and ^{13}C NMR data were recorded at 25°C on Bruker AM 400 or 700 instruments, operating at 400 MHz for ^{1}H and 100 MHz for ^{13}C nuclei or 700 MHz for ^{1}H and 175 MHz for ^{13}C nuclei, respectively. ^{1}H and ^{13}C NMR chemical shifts were referenced to residual solvent signals: δ_H 7.26 and δ_C 77.16 for $CDCl_3$; δ_H 3.31 and δ_C 49.00 for CD_3OD; δ_H 4.79 for D_2O. ^{1}H-^{1}H COSY, HSQC, and HMBC were performed using standard Bruker pulse sequences. Optical rotations were measured with an AUTOPOL®IV automatic polarimeter (Rudolph Research Analytical, Hackettstown, NJ) using a quartz cell with 1 mL capacity and 10 cm path length. Electrospray ionization mass spectrometry (ESI-MS) was carried out with a Varian 500-MS IT LC-MS (ESI) using soft positive ionization. High resolution ESI-MS analyses were acquired with an LTQ orbitrap (Thermo). Analytical HPLC was carried out with a Varian system equipped with Prostar 210 pumps and a photodiode array (PDA) detector or Agilent 1260 infinity system equipped with quaternary pumps and a DAD detector. Semipreparative HPLC was carried out on a Varian system equipped with Prostar 210 pumps and a PDA detector. Analytical HPLC was conducted using an Altima C-18 column (5 µm, 250 x 4.6 mm, Grace Davison Discovery Sciences, Deerfield, IL). Semipreparative HPLC was conducted using an Altima C-18 column (5 µm, 250 x 10 mm, Grace Davison Discovery Sciences). Preparative HPLC was performed on Agilent 1260 Infinity system equipped with prep pump and an Agilent Eclipse XDB-C18 column (7 µm, 250 x 21.2 mm). Protein purification was conducted on Äkta FPLC (Pharmacia Amersham Biotech, Uppsala, Sweden).

Chemicals and materials: Column chromatography was performed either on silica gel (230–400 mesh, Natland International Corporation, Morrisville, NC) or Sephadex LH-20 (GE Healthcare, Glies, UK). Dowex-50Wx2 and XAD-16 resins were purchased from the Alfa Aesar (Ward Hill, MA) and Sigma-Aldrich (St. Louis, MO), respectively. Thionyl chloride, (*R*)-(-)- or (*S*)-(+)-methoxy-trifluoromethylphenylacetic acid chlorides (MTPACls), chlorotitaniumtri-*iso*-propoxide, and *m*CPBA were purchased from Alfa Aesar. NaH, anhydrous methanol, trifluoroacetic anhydride, and methyl acetate were purchased from ACROS Organics (Pittsburgh, PA), and 5-hydroxy-2-methylpyridine, 4-methoxybenzyl chloride, Dess-Martin periodinane, (1*R*,2*S*,5*R*)-(−)-methyl-(*S*)-p-toluenesulfinate, LiHMDS, and LDA were purchased from Sigma-Aldrich. Buffer components and all other common biochemicals and chemicals were purchased from standard commercial sources. Restriction enzymes, T4 DNA ligase and dNTPs (New England Biolabs, Ipswich, MA), T4 DNA polymerase (Lucigen, Middleton, WI), and Platinum Pfx DNA polymerase (Invitrogen, Carlsbad, CA) were purchased. *E. coli* NovaBlue and BL21(DE3) cells were from Novagen (Madison, WI). Synthetic DNA oligonucleotides were purchased from Integrated DNA Technologies, Inc (Coralville, IW). DNA sequencing was performed by Genewiz, Inc (Research Triangle Park, NC).

Bioinformatics analysis of KedY4

Selected MIO-containing aminomutases, whose functions have been confirmed experimentally, were subjected to sequence alignment with ClustalW2 (Fig. S1). The highly conserved ASG motif for MIO formation and the other conserved active-site residues are marked in blue. Residues directly involved in L-tyrosine specificity in TAMs are marked in red (1). All the active sites assignments were based on the crystal structure and structural modeling of SgcC4 (2-4).

Expression and overproduction in *E. coli* and purification of KedY4

Construction of the *kedY4* expression plasmid pBS16013. To construct the *kedY4* expression plasmid pBS16013, *kedY4* was PCR amplified from pBS16005 (5) and cloned into pBS3080 using ligation independent cloning techniques to afford pBS16013. Briefly, pBS3080 was first digested with *Bsm*FI and purified by gel electrophoresis. The linearized vector was treated with T4 DNA polymerase in the presence of dGTP at 20°C for 30 min followed by heating at 75°C for 20 min to denature the polymerase, affording overhangs with complimentary sequences to clone the PCR amplified *kedY4*.

The *kedY4* gene was amplified by PCR from pBS16005, using the primers 5′-AAAACCTCTATTTCCAGTCGCCGGCCGAGACGACCTCCCAGG-3′ and 5′-TACTTACTTAAATGTTAGCGCAGCGTCACCGAGTGCTCCGC-3′, purified by gel electrophoresis, and treated with T4 DNA polymerase in the presence of dCTP at 20°C for 30 min followed by heating at 75°C. The linearized and T4 DNA polymerase treated pBS3080 vector and the PCR amplified and T4 DNA polymerase treated *kedY4* fragment were then mixed at room temperature, annealed on ice for 5 min, and transformed into *E. coli* NovaBlue for ligation independent cloning to construct the *kedY4* expression plasmid pBS16013. Finally, pBS16013 was isolated from *E. coli* NovaBlue and confirmed by DNA sequencing, in which KedY4 is produced as a fusion protein with an N-terminal His_6-tag that is cleavable by TEV protease. Upon TEV cleavage, the resultant KedY4 lacks the first three N-terminal residues and contains a Thr4Ser mutation.

KedY4 overproduction in *E. coli*. pBS16013 was introduced into *E. coli* BL21(DE3) by transformation, and the resultant recombinant strains were grown overnight in 50 mL of LB containing 2 mM $MgSO_4$ and 50 µg/mL kanamycin. A 10 mL aliquot of the overnight culture was used to inoculate 1 L of LB containing 2 mM $MgSO_4$ and 50 µg/mL kanamycin, which was then incubated at 37°C with shaking at 250 rpm. Once the OD_{600} reached ~0.4, the temperature was reduced to 18°C. After the cultures reached thermal equilibrium, gene expression was induced by the addition of isopropyl β-D-thiogalactopyranoside (IPTG) to 50 µg/mL, and incubation continued for an additional 16 hrs at 18°C. *E. coli* cells were harvested by centrifugation at 3,500 x g and 4°C for 20 min.

Purification of KedY4. The *E. coli* cell pellets, carrying the pBS16013 expression construct, were resuspended in lysis buffer (1 µg/mL DNAse, 300 mM NaCl, 10 mM imidiazole, 5% glycerol, and 50 mM Tris-HCl, pH 8.0), sonicated (30 × 2 s on ice), and clarified by centrifugation at 15,000 x g and 4°C for 30 min. Supernatant was applied to a 5 mL HisTrap HP column (GE Healthcare, Uppsala, Sweden) and washed with lysis buffer using an Äkta FPLC. Wash buffer (300 mM NaCl, 20 mM imidiazole, 50 mM Tris-HCl, pH 8.0) was used to further remove contaminants, and proteins were eluted with wash buffer containing 250 mM imidiazole. Proteins were immediately desalted by passing through a HiPrep 26/10 desalting column (GE Healthcare) equilibrated with 10 mM triethanolamine-HCl, pH 8.0, 10 mM NaCl, concentrated and frozen in small aliquots with liquid nitrogen, and stored at -80°C. Alternatively, proteins were immediately diluted from 5 mL to 15 mL buffer A (50 mM Tris-HCl, pH 8.0, 10 mM NaCl) plus 1 mM dithiothreitol, 0.1 mM EDTA, and 50 µg/mL TEV protease bearing a C-terminal His_6-tag and incubated overnight. The TEV cleaved samples were further diluted to 50 mL with buffer A and passed over a Ni-Sepharose 6 fast flow column to remove the TEV protease, and the flowthrough was then loaded onto a MonoQ 10/80 column (GE Healthcare). A linear gradient over 12 column volumes from 10 % buffer B to 50 % buffer B (50 mM Tris-HCl, pH 8.0, 1.0 M NaCl) was used to elute the proteins. Purity of protein from the fractions was analyzed by SDS-PAGE (Fig. S2), and the calculated MW for the His_6-tagged KedY4 and TEV-cleaved KedY4 are 59661.1 Da and 57212.6 Da, respectively. Pure fractions were pooled, concentrated, buffer exchanged into 10 mM triethanolamine-HCl, pH 8.0, with 10 mM NaCl, frozen in small aliquots with liquid nitrogen, and stored at -80°C.

Fermentation and isolation of 2-aza-L-tyrosine from *Streptomyces chibaensis* SF-1346

Production and isolation of 2-aza-L-tyrosine from *S. chibaensis* SF-1346 essentially followed literature procedures (6). Thus, 10 µL of spore suspension of *S. chibaensis* SF-1346 was inoculated into a 250 mL flask containing 50 mL of the ISP2 broth, followed by shaking (250 rpm) continuously for 2 days at 28.0°C to prepare the seed inoculum. The production fermentation was accomplished by adding the inoculum 20 mL into 2-L flasks containing 400 mL (20 × 0.4 L) of the production culture broth [Malt extract (20.0 g), soybean flour (20.0 g), peptone (5.0 g), pharmamedia (10.0 g), soybean oil (3 g), $FeSO_4$ (10 mg), $NiCl_2$ (1 mg), $CoCl_2$ (1 mg) in a final volume of 1.0 L H_2O, pH 7.0], and then shaking (250 rpm) for 4 days at 28.0°C . The harvested broth was filtrated through two layers of filter paper with celite. The pH value of the resultant supernant was adjusted to 2 using 5 N HCl, and then, 200 g Dowex-50Wx2 resin was added and stirred for 1 hr. The resin was recovered by filtration through the

cheese cloth. The resin was then washed with 1 L pH 2 water and eluted with 500 mL1 N NH_3•H_2O. The ammonia of 1 N NH_3•H_2O elutant was removed by evaporator. XAD-16 resin (10 g) was added to the solution and stirred for 30 min. The secondary metabolites were extracted by 5% methanol water (100 mL) from XAD-16 resin. The 100 mL elutant was evaporated to dryness to give the dark residue, which was dissolved in 5 ml 50% methanol water and subjected to the Sephadex LH-20 column eluted with 50% methanol. Then, HPLC detection of 2-aza-L-tyrosine was performed on an analytical C-18 reversed phase column. All the fractions that contained 2-aza-L-tyrosine were combined. Finally, 34 mg of 2-aza-L-tyrosine was further purified by semipreparative HPLC using a gradient 0% CH_3CN (0-5 min), from 0% to 5% CH_3CN (5-10 min), then 100% CH_3CN to wash the column with a flow rate at 3.8 mL/ min.

Spectroscopic data of 2-aza-L-tyrosine: $[\alpha]_D^{26.1}$ +51.2 (*c* 0.5, 1 N HCl). ESI-MS (positive ion) for the $[M + H]^+$ ion at *m*/*z* 183. ^{1}H NMR in D_2O, δ 3.99 (1H, dd, *J* = 4.8, 8.0 Hz, H-2′), 3.25 (1H, dd, *J* = 4.8, 14.8 Hz, H-3′a), 3.12 (1H, dd, *J* = 8.0, 14.8 Hz, H-3′b), 7.18 (1H, d, *J* = 8.8 Hz, H-6), 7.24 (1H, dd, *J* = 2.8, 8.8 Hz H-5), 8.02 (1H, d, *J* = 2.8 Hz, H-3). ^{13}C NMR in D_2O, δ 175.6 (s, C-1′), 159.0 (s, C-4), 142.1 (s, C-1), 138.7 (d, C-3), 126.9 (d, C-6), 125.3 (d, C-5), 37.3 (t, C-3′), 55.6 (d, C-2′) (Figs. S3 and S4).

In vitro characterization of KedY4 as an MIO-containing aminomutase

KedY4 activity assays. Standard reaction conditions consisted of 100 mM Bis-tris-propane (BTP), pH 8.5, with 50 mM KCl, 20 μM enzyme and 2 mM substrate in 50 μL, with incubation at 25°C for 4 hours. The reactions were initiated by the addition of KedY4 and terminated by the addition of 25 μL of 1.0 M TFA, and protein was precipitated by centrifugation at 16,000 x g for 5 minutes. The supernatant was neutralized by addition of 25 μL of 1.0 M NaOH and subjected to the HPLC analysis with an Atima C-18 column (5 μm, 4.6 x 250 mm, Grace Davison Discovery Sciences). The linear gradients were developed from 0.1 M ammonium acetate in water (A) to acetonitrile (B) in the following manner (beginning time and ending time with linear increase to % B): 0 min, 1% B; 0−5 min, 5% B; 5−15 min, 25% B; 15−18 min, 25% B; and 18−19 min, 1% B. The flow rate was kept constant at 1.0 mL/min, and elution was monitored at 280 nm.

To determine the pH dependence of KedY4, 1 mM 2-aza-L-tyrosine was added to 0.625 μM KedY4 in 50 mM KCl and 100 mM BTP at various pHs (6.5, 7.0, 7.5, 8.0, 8.5, 9.0, 9.5, and 10.0) and 100 mM CAPS at pHs (10.5 and 11.0) in 50 μL reactions and incubated for 1 hour at 25°C (Fig. S24).

Determination of the kinetic parameters of KedY4. The steady-state constants of KedY4-catalyzed formation of (*R*)-2-aza-β-tyrosine and 2-aza-4-hydroxycinnamic acid from 2-aza-L-tyrosine were determined using the single-point methodology. Preliminary experiments established that the KedY4-catalyzed reaction was linear over a period of 60 min. All single-point kinetic assays were therefore based on an incubation time of 30 min. Nine assays with each volume of 50 μL in assay buffer (100 mM BTP, 50 mM KCl, pH 8.5) and 2-aza-L-tyrosine with variable final concentrations (2.0, 1.0, 0.5, 0.25, 0.125, 0.10, 0.075, 0.050, 0.025 mM) were pre-incubated at 25 °C for 5 min. The reactions were initiated by adding 2.45 μL of 12.75 μM KedY4 (0.625 μM KedY4 final concentration) and incubated at 25°C for 30 min followed by quenching with 25 μL 1.0 M TFA. The protein was precipitated by centrifugation at 16,000 x g for 5 minutes. Then, the supernatant was neutralized by addition of 25 μL 1.0 M NaOH. The resulting mixtures were subjected to HPLC-UV/Vis analysis using the Agilent 1260 infinity system with an Atima C-18 column (5 μm, 4.6 mm x 250 mm, Grace Davison Discovery Sciences). The linear gradient was developed from 0.1% TFA in water (A) to 0.1% TFA in acetonitrile (B) in the following manner: 0-3 min, 0% B; 3−15 min, 0%-35% B; 15.1−18 min, 100% B; and 18.1−23 min, 0% B. The flow rate was kept constant at 1.0 mL/min, and elution was monitored at 280 nm. Each reaction was repeated twice. A standard curve of enzymatically prepared (*R*)-2-aza-β-tyrosine and 2-aza-4-hydroxycinnamic acid was employed for quantification. Steady-state kinetic constants were extracted by fitting the Michaelis-Menten equation to the data by non-linear regression using Kaleida Graph by Synergy Software (Reading, PA). For the reverse reaction, nine assays with each

volume of 50 µL in assay buffer (100 mM BTP, 50 mM KCl, pH 8.50) and (*R*)-2-aza-β-tyrosine with variable final concentrations (4.0, 2.0, 1.0, 0.50, 0.25, 0.20, 0.15, 0.10, 0.050 mM) were processed in the same way as that of forward reaction.

Large scale enzymatic synthesis, purification, and characterization of (*R*)-2-aza-β-tyrosine (Fig. S25)

Enzymatic synthesis of (*R*)-2-aza-β-tyrosine from 2-aza-L-tyrosine. KedY4-catalyzed scale-up synthesis of (*R*)-2-aza-β-tyrosine using 2-aza-L-tyrosine as a substrate was achieved in a 75-mL reaction mixture containing 100 mM BTP, pH 8.5, 50 mM KCl, 2.5 mM 2-aza-L-tyrosine and 25 µM KedY4. The reaction mixture was shaken at 25°C. After 4 hr incubation, the reaction was quenched by adding 30 mL 1.0 M TFA to precipitate all proteins. The resulting supernatant was transferred to another tube, and the pH was adjusted to 8.5 with 1.0 M NaOH. The resulting solution was lyophilized to dryness. The crude products were then dissolved in 5 mL water and purified by using a semipreparative HPLC column eluting with a gradient from 1% to 4% CH_3CN water (0 - 4 min), then from 4% to 25% CH_3CN water (4 - 10 min), 75% CH_3CN for 5 min in a flow rate of 4 mL/min, yielding 2.6 mg of (*R*)-2-aza-β-tyrosine and 5.1 mg of 2-aza-hydroxycinnamic acid, respectively. Under these conditions, both compounds were purified as BTP-complexes.

Spectroscopic data of (*R*)-2-aza-β-tyrosine as a BTP complex: $[\alpha]_D^{26.1}$ +4.1 (*c* 0.08, H_2O). ESI-MS (positive ion) for the $[M + H]^+$ ion at *m*/*z* 183, and HR-ESI-MS (positive ion) for the $[M + H]^+$ ion at *m*/*z* 183.0762 (the calculated $[M + H]^+$ ion for $C_8H_{10}N_2O_3$ at *m/z* 183.0764). ^{1}H NMR in D_2O, δ 3.99 (2H, d, *J* = 6.9 Hz, H-2′); 3.25 (1H, t, *J* = 6.9 Hz, H-3′); 7.28 (1H, overlapped, H-6); 7.28 (1H, overlapped, H-5); 8.10 (1H, brs, H-3). ^{13}C NMR in D_2O, δ 177.1 (s, C-1′), 152.9 (s, C-4), 145.8 (s, C-1), 137.7 (d, C-3), 124.4 (d, C-5), 123.1 (d, C-6), 52.3 (d, C-3′), 39.7 (t, C-2′) (Figs. S26-S30).

Spectroscopic data of 2-aza-hydroxycinnamic acid as a BTP complex: ESI-MS (positive ion) for the $[M + H]^+$ ion at *m*/*z* 166, and HR-ESI-MS (positive ion) for the $[M + H]^+$ ion at *m*/*z* 166.0496 (the calculated $[M + H]^+$ ion for $C_8H_8NO_3$ at *m/z* 166.0498). ^{1}H NMR in CD_3OD, δ 6.65 (1H, d, *J* = 15.8 Hz, H-2′); 7.46 (1H, d, *J* = 15.8 Hz, H-3′); 7.49 (1H, d, *J* = 8.8 Hz, H-6); 7.21 (1H, dd, *J* = 8.8, 2.8 Hz, H-5); 8.11 (1H, d, *J* = 2.8 Hz, H-3). ^{13}C NMR in CD_3OD, δ 173.7 (s, C-1′), 156.1 (s, C-4), 146.4 (s, C-1), 141.2 (d, C-3′), 138.9 (d, C-3), 124.4 (d, C-6), 125.5 (d, C-5), 124.4 (d, C-2′) (Figs. S31 and S32).

Conversion of the enzymatically prepared (*R*)-2-aza-β-tyrosine to (*R*)-2-aza-β-tyrosine methyl ester. In an oven dried 5 mL round bottom flask equipped with magnetic stir bar, argon inlet and a rubber septum, the enzymatically synthesized (*R*)-2-aza-β-tyrosine (2.6 mg) was dissolved in anhydrous MeOH (0.5 mL). Thionyl chloride (5 µL) was added at room temperature and the mixture was stirred for 2 hrs. The mixture was quenched with 5 µL water and stirred for an additional 5 min. The solvent was removed on a rotary evaporator. The crude product was purified by semipreparative HPLC (8% CH_3CN in water with 0.1% TFA) to give (*R*)-2-aza-β-tyrosine methyl ester as its TFA salt (1.0 mg) as white powder.

Spectroscopic data of (*R*)-2-aza-β-tyrosine methyl ester: $[\alpha]_D^{26.1}$ +3.3 (*c* 0.06, MeOH). ESI-MS (positive ion) for the $[M + H]^+$ ion at *m*/*z* 197, and HR-ESI-MS (positive ion) for the $[M + H]^+$ ion at *m*/*z* 197.0920 (the calculared $[M + H]^+$ ion for $C_9H_{14}N_2O_3$ $[M + H]^+$ at *m/z* 197.0947). ^{1}H NMR in CD_3OD, δ 3.03 (2H, dd, *J* = 6.8, 3.3 Hz, H-2′); 4.74 (1H, t, *J* = 6.8 Hz, H-3′); 3.70 (3H, s, OMe,); 7.23 (1H, dd, *J* = 2.8, 8.4 Hz, H-5); 7.32 (1H, brd, *J* = 8.4 Hz, H-6); 8.19 (1H, brd, *J* = 2.8 Hz, H-3). ^{13}C NMR in CD_3OD, δ 171.8 (s, C-1′), 155.8 (s, C-4), 146.1 (s, C-1), 139.0 (d, C-3), 124.5 (d, C-6), 124.3 (d, C-5), 52.7 (q, OMe), 52.3 (d, C-3′), 38.7 (t, C-2′) (Figs. S33 and S34).

Synthesis of the Mosher amide (*S*)-MTPA of (*R*)-2-aza-β-tyrosine methyl ester from enzymatically generated (*R*)-2-aza-β-tyrosine methyl ester. These syntheses were carried out by following literature procedures (7, 8). Thus, in an oven dried 5 mL round bottom flask equipped with

magnetic stir bar, argon inlet and a rubber septum, enzymatically synthesized (*R*)-2-aza-β-tyrosine methyl ester (~0.7 mg) was dissolved in anhydrous CH_2Cl_2 (0.3 mL). Anhydrous triethylamine (4 µL) and (*R*)-(-)-methoxy-trifluoromethylphenylacetic acid chloride (MTPACl, 5 µL) were added sequentially at room temperature and the mixture was stirred for 3 hrs. The mixture was quenched with 10 µL water and stirred for an additional 10 min, then diluted with CH_2Cl_2 (1.5 mL). The solvent was removed on a rotary evaporator. The crude product was purified by the preparative TLC (60% EtOAc in hexanes) to give (*S*)-MTPA of (*R*)-2-aza-β-tyrosine methyl ester as a gummy material (~0.8 mg).

Spectroscopic data of (*S*)-MTPA of (*R*)-2-aza-β-tyrosine methyl ester: ESI-MS (positive ion) for the $[M + H]^+$ ion at *m*/*z* 629 $[M + H]^+$, and HR-ESI-MS (positive ion) for the $[M + H]^+$ ion at *m*/*z* 629.1704 (the calculated $[M + H]^+$ for $C_{29}H_{27}F_6N_2O_7$ at *m/z* 629.1717). ^{1}H NMR in $CDCl_3$, δ 2.87 (1H, dd, *J* = 6.6, 16.0 Hz, H-2′a); 3.05 (1H, dd, *J* = 5.6, 16.0 Hz, H-2′b), 3.38 (3H, brs, OMe), 3.58 (3H, s, OMe), 3.68 (3H, brs, OMe), 5.57 (1H, m, H-3′); 7.40-7.64 (12H, overlapped); 8.11 (1H, brd, *J* = 8.6 Hz, NH); 8.40 (1H, d, *J* = 2.4 Hz, H-3) (Figs. S35-S38).

Synthesis of the Mosher amide (*R*)-MTPA of (*R*)-2-aza-β-tyrosine methyl ester from enzymatically generated (*R*)-2-aza-β-tyrosine methyl ester. In an oven dried 5 mL round bottom flask equipped with magnetic stir bar, argon inlet and a rubber septum, enzymatically synthesized (*R*)-2-aza-β-tyrosine methyl ester (~0.2 mg) was dissolved in anhydrous CH_2Cl_2 (0.2 mL). Anhydrous triethylamine (2 µL) and (*S*)-(+)-methoxy-trifluoromethylphenylacetic acid chloride (MTPACl, 3 µL) were added sequentially at room temperature and the mixture was stirred for 3 hrs. The mixture was quenched with 5 µL water and stirred for an additional 10 min, then diluted with CH_2Cl_2 (1 mL). The solvent was removed on a rotary evaporator. The crude product was purified by preparative TLC (60% EtOAc in hexanes) to give (*R*)-MTPA of (*R*)-2-aza-β-tyrosine methyl ester as a gummy material (~0.2 mg).

Spectroscopic data of (*R*)-MTPA of (*R*)-2-aza-β-tyrosine methyl ester: ESI-MS (positive ion) for the $[M + H]^+$ ion at *m*/*z* 629, and HR-ESIMS (positive ion) for the $[M + H]^+$ ion at *m*/*z* 629.1702 (the calculated $[M + H]^+$ ion for $C_{29}H_{27}F_6N_2O_7$ at *m/z* 629.1717). ^{1}H NMR in $CDCl_3$, δ 2.97 (1H, dd, *J* = 7.1, 16.3 Hz, H-2′a); 3.12 (1H, dd, *J* = 5.7, 16.3 Hz, H-2′b), 3.44 (3H, brs, OMe), 3.65 (3H, s, OMe), 3.67 (3H, brs, OMe), 5.57 (1H, m, H-3′); 7.32-7.62 (12H, overlapped); 8.26 (1H, brd, *J* = 8.3 Hz, NH); 8.44 (1H, d, *J* = 2.5 Hz, H-3) (Figs. S39-S42).

Chemical synthesis of (*R*)- and (*S*)-2-aza-β-tyrosine, their methyl esters, and their (*R*)- and (*S*)-MTPAs as authentic standards or alternative substrates (Fig. S5)

Both the syntheses of (*R*)- and (*S*)-2-aza-β-tyrosine and their methyl esters (9) and conversion of (*R*)- and (*S*)-2-aza-β-tyrosine methyl esters into their (*R*)- and (*S*)-MTPAs (7, 8) were carried out by following literature procedures.

Synthesis of 5-[(4-methoxybenzyl)oxy]-2-methylpyridine (2): NaH (60% dispersion in mineral oil, 2.7 g, 1.3 equiv.) was added to a 0°C cooled solution of 5-hydroxy-2-methylpyridine (**1**) (5.5 g) in anhydrous DMF (50 mL) in four portions under argon over a period of 45 min. After stirring the mixture for 55 min, 4-methoxybenzyl chloride (8.1 mL, 1.2 equiv.) was added dropwise via a syringe and the resultant mixture was stirred for an additional 3 hrs at 0°C. The reaction mixture was then quenched with MeOH (3 mL) at 0°C and diluted with EtOAc (500 mL). The mixture was washed with brine (4 × 100 mL), dried ($MgSO_4$, and the solvent was removed on a rotary evaporator. The crude product was purified by silica gel column chromatography (10% EtOAc in hexanes) to afford **2** as a colorless viscous oil (8.90 g, 78%) (Figs. S6 and S7).

Synthesis of 2-hydroxymethyl-5-[(4 methoxybenzyl)oxy]pyridine (3): *m*-Chloroperoxybenzoic acid (55% max, 12 g, around 1.5 equiv.) was added to a solution of **2** (7.6 g) in $CHCl_3$ (200 mL) at room temperature and the reaction mixture was stirred for 2 hrs. The mixture was then quenched with

aqueous Na_2SO_3 (6.3 g, 1.5 equiv., in 34 mL of water) and stirred for 30 min. The mixture was diluted with $CHCl_3$ (150 mL), washed with water (100 mL), 4% aqueous $NaHCO_3$ (2×80 mL), dried ($MgSO_4$) and the solvent was removed on a rotary evaporator and dried by lyophilizer overnight. The resulting crude product (9.1 g, white solid) was dissolved in CH_2Cl_2 (100 mL), and trifluoroacetic anhydride (10 mL, 67 mmol, 2.1 equiv.) was added at room temperature under argon. After stirring the mixture for 17 hrs, MeOH (66 mL) was added at room temperature and stirred for an additional 15 min. The mixture was concentrated on a rotary evaporator, and the residue was diluted with EtOAc (200 mL), washed with 10% aqueous $NaHCO_3$ (2×75 mL), and dried over (Na_2SO_4). The solvent was removed on a rotary evaporator, and the crude compound was purified by silica gel column chromatography (20% EtOAc in hexanes to pure EtOAc) to afford **3** as a white solid (6.2 g, 76%) (Figs. S8 and S9).

Synthesis of 5-[(4-methoxybenzyl)oxy]-2-pyridinecarbaldehyde (4): Dess-Martin periodinane (DMP) (7.0 g, 1.16 equiv.) and $NaHCO_3$ (5.5 g, 2 equiv.) was added to the above prepared **3** (3.5 g) in CH_2Cl_2 (130 mL) at room temperature, the mixture was stirred for 30 min, and isopropanol (2 mL) was added for additional 10 min. The reaction mixture was then filtered over celite powder and washed with CH_2Cl_2 (10 mL). The filtrate was concentrated on a rotary evaporator, and the residue was purified by silica gel column chromatography (5–20% EtOAc in hexanes) to afford **4** as a white solid (3.15 g, 90%) (Figs. S10 and S11).

Synthesis of (*S*)-(+)-*N*-((1*E*)-{5-[(4-methoxybenzyl)oxy]-2-pyridinyl}methylidene)-4 methylbenzenesulfinamide (5): In an oven dried 250 mL round bottom flask equipped with magnetic stir bar, argon inlet and a rubber septum, (1*R*,2*S*,5*R*)-(–)-menthyl-(*S*)-p-toluenesulfinate (Andersen reagent) (2.83 g, 1.0 equiv.) was dissolved in anhydrous THF (30 mL). The mixture was cooled to −78°C (dry ice–acetone bath), and a solution of LiHMDS (1.0 M solution in THF, 12.8 mL, 1.3 equiv.) was added dropwise via a syringe. After stirring the mixture for 15 min at −78°C, the cooling bath was removed, the mixture allowed to warm to room temperature, and stirring was continued for additional 4 hrs. The reaction mixture was then cooled to −78°C, and a solution of **4** (2.34 g, 1.0 equiv.) in anhydrous THF (20 mL) was added dropwise via a syringe. After stirring the mixture for 6 hrs at −78°C, it was allowed to warm to room temperature and stirred for additional 10 hrs. The reaction was then cooled to −78°C and quenched with water (10 mL). The mixture was diluted with EtOAc (250 mL) and water (25 mL). The organic layer was separated, and the aqueous layer was extracted with EtOAc (100 mL). The combined organic layers were washed with brine (2×80 mL), dried over ($MgSO_4$), and the solvent was removed on a rotary evaporator. The crude compound was purified by silica gel column chromatography (10–20% EtOAc in hexanes) to afford **5** as a yellow powder (2.3 g, 62%) (Figs. S12 and S13).

Synthesis of (S_s,*R*)- and (S_s,*S*)-methyl 3-{5-[(4-methoxybenzyl)oxy]-2-pyridinyl}-3-{[(4-methylphenyl)-sulfinyl]amino}propanoates (6a and 6b): In an oven dried 50 mL round bottom flask equipped with magnetic stir bar, argon inlet, and a rubber septum, a mixture of lithium di-*iso*-propylamide mono(tetrahydrofuran) (1.5 M solution in cyclohexane, 1.4 mL, 1.3 equiv.) and THF (5 mL) was cooled to −78°C (dry ice–acetone bath). Methyl acetate (0.16 mL, 1.3 equiv.) was added, and the mixture was stirred for 50 min. A solution of chlorotitaniumtri-*iso*-propoxide (1.0 mL, 2.6 equiv.) in THF (3 mL) was added to the lithium enolate solution at −78°C. The resulting lemon yellow solution was stirred for 45 min, and a solution of **5** (0.620 g) in THF (4 mL) was added dropwise. The reaction mixture was stirred for additional 3.5 hrs at −78°C, quenched with a saturated NH_4Cl solution (4 mL) at −78°C, and the mixture was allowed to warm to room temperature. The mixture was diluted with EtOAc (200 mL) and water (100 mL). The organic layer was separated, and the aqueous layer was extracted with EtOAc (2×120 mL). The combined organic layers were washed with brine (2×80 mL), dried over ($MgSO_4$), and the solvent was removed on a rotary evaporator. The crude products [diastereomeric ratio of (S_s,*R*)- and (S_s,*S*)-methyl 3-{5-[(4-methoxybenzyl)oxy]-2-pyridinyl}-3-{[(4-methylphenyl)-sulfinyl]amino}propanoates (**6a**:**6b** = 4:1)] were purified by silica gel column chromatography (10–50% EtOAc in hexanes) to afford a mixture of **6a** and **6b**, (0.56 g, 75%). The latter mixture was finally dissolved in 5 mL MeCN/H_2O (3:1) and separated by preparative reversed-phase HPLC

(MeCN:H_2O/45:55, 20 mL/min). The compound was collected, concentrated on a rotary evaporator (bath temperature: <35°C), and lyophilized to afford **6a** (0.420 g, 60%) and **6b** as colorless gum (0.11 g, 15%) (Figs. S14-S17).

Synthesis of (*R*)- and (*S*)-2-aza-β-tyrosine methyl ester: Trifluoroacetic acid (0.36 mL, 5.0 equiv.) was added to a 0°C cooled solution of **6a** (0.40 g) and anhydrous methanol (16 mL) under argon, and the mixture was stirred for 5 hrs. After completion of the reaction, as determined by HPLC, the solvent was removed on a rotary evaporator. The residue was dissolved in water (25 mL) and ethyl ether (25 mL). The aqueous layer was separated, and the organic layer was extracted with water (20 mL). The combined aqueous layer was washed with ethyl ether (2×25 mL) and concentrated on a rotary evaporator. The residue was dried by lyophilizer over 12 hrs to afford crude product. This crude product was dissolved in anhydrous CH_2Cl_2 (17 mL), and trifluoroacetic acid (1.33 mL, 20.0 equiv.) was added at room temperature under argon. The mixture was stirred for 3 hrs, and the resulting solution was concentrated on a rotary evaporator. The colorless residue was dissolved in CH_3CN–0.1% aq TFA (1:3 ratio, 5 mL) and purified by preparative reverse phase HPLC using MeCN:0.1% aqueous trifluoroacetic acid/8:92, 20 mL/min at 270 nm. Evaporation and lyophilization of the product afforded (*R*)-2-aza-β-tyrosine methyl ester as its TFA salt (230 mg) (Figs. S18 and S19). $[\alpha]_D^{26.9}$ = +3.8 (c = 1.0, in MeOH).

Trifluoroacetic acid (0.1 mL, 5.0 equiv.) was added to a 0°C cooled solution of **6b** (0.10 g) and anhydrous methanol (5 mL) under argon, and the mixture was stirred for 5 hrs. After completion of the reaction, as determined by HPLC, the solvent was removed on a rotary evaporator. The residue was dissolved in water (7 mL) and ethyl ether (7 mL). The aqueous layer was separated, and the organic layer was extracted with water (7 mL). The combined aqueous layer was washed with ethyl ether (2×7 mL) and concentrated on a rotary evaporator. The residue was dried by lyophilizer over 12 hrs to afford a crude product. This crude product was dissolved in anhydrous CH_2Cl_2 (5 mL), and trifluoroacetic acid (0.33 mL, 20.0 equiv.) was added at room temperature under argon. The mixture was stirred for 3 hrs, and the resulting violet solution was concentrated on a rotary evaporator. The colorless residue was dissolved in CH_3CN–0.1% aq TFA (1:3 ratio, 2 mL) and purified by preparative reverse phase HPLC using CH_3CN:0.1% aqueous trifluoroacetic acid/8:92, 20 mL/min at 270 nm. Evaporation and lyophilization of the product afforded (*S*)-2-aza-β-tyrosine methyl ester as its TFA salt (60 mg). $[\alpha]_D^{26.9}$ = -3.3 (c = 1.0, in MeOH).

Synthesis of (*R*)- and (*S*)-2-aza-β-tyrosine: To 24 mg of (*R*)-2-aza-β-tyrosine methyl ester in 0.5 mL of THF was added 2 mL of a 2:2:1 mixture of MeOH:THF:H_2O at 0°C. To the solution was then added 11.5 mg powdered LiOH (5 equiv.) at 0°C. The resulting mixture was allowed to warm to room temperature over the course of 3 hrs and then centrifuged to remove the insoluble solid. The volatiles of the supernatant were removed by rotary evaporation with gentle heating. The basic aqueous layer was acidified with 10% TFA (final pH 3-4), and the mixture was further purified by reversed phase HPLC using 5% CH_3CN in water containing 0.1% TFA with a flow rate at 3.8 mL/min to yield 16 mg (*R*)-2-aza-β-tyrosine as its TFA salt (16 mg, 73%) (Figs. S20-S23). $[\alpha]_D^{26.9}$ = +4.6 (c = 1.0, in H_2O).

To 24 mg of (*S*)-2-aza-β-tyrosine methyl ester in 0.5 mL of THF was added 2 mL of a 2:2:1 mixture of MeOH:THF:H_2O at 0°C. To the solution was then added 11.5 mg powdered LiOH (5 equiv.) at 0°C. The resulting mixture was allowed to warm to room temperature over the course of 3 hrs and then centrifuged to remove the insoluble solid. The volatiles of the supernatant were removed by rotary evaporation with gentle heating. The basic aqueous layer was acidified with 10% TFA (final pH 3-4), and the mixture was further purified by reversed phase HPLC using 5% CH_3CN in water containing 0.1% TFA with a flow rate at 3.8 mL/min to yield 15 mg (*S*)-2-aza-β-tyrosine as its TFA salt (15 mg, 68%). $[\alpha]_D^{26.9}$ = -4.3 (c = 1.0, in H_2O).

Synthesis of the Mosher amides (*R*)- and (*S*)-MTPAs of (*S*)-2-aza-β-tyrosine methyl ester from synthetic (*S*)-2-aza-β-tyrosine methyl ester. In an oven dried 10 mL round bottom flask equipped

with magnetic stir bar, argon inlet and a rubber septum, the chemically synthesized (*S*)-2-aza-β-tyrosine methyl ester (6 mg) was dissolved in anhydrous CH_2Cl_2 (0.5 mL). Anhydrous triethylamine (18 µL, 6 equiv.) and (*R*)-(-)-methoxy-trifluoromethylphenylacetic acid chloride (MTPACl, 18 µL, 3.0 equiv.) were added sequentially at room temperature, and the mixture was stirred for 3 hrs. The mixture was quenched with 10 µL water and stirred for an additional 10 min, then diluted with CH_2Cl_2 (2 mL). The solvent was removed on a rotary evaporator. The crude product was purified by the preparative TLC (60% EtOAc in hexanes) to (*S*)-MTPAs of (*S*)-2-aza-β-tyrosine methyl ester as a gummy material (7.8 mg). ESI-MS (positive ion) for the $[M + H]^+$ ion at *m*/*z* 629, and HR-ESI-MS (positive ion) for the $[M + H]^+$ ion at *m*/*z* 629.1702 (the calculated $[M + H]^+$ ion for $C_{29}H_{27}F_6N_2O_7$ at *m/z* 629.1717). ^{1}H NMR in $CDCl_3$, δ 2.92 (1H, dd, *J* = 6.7, 16.1 Hz, H-2′a); 3.12 (1H, dd, *J* = 5.4, 16.1 Hz, H-2′b), 3.44 (3H, brs, OMe), 3.64 (3H, s, OMe), 3.67 (3H, brs, OMe), 5.55 (1H, m, H-3′); 7.32-7.64 (12H, overlapped); 8.08 (1H, brd, *J* = 8.7 Hz, NH); 8.37 (1H, d, *J* = 2.6 Hz, H-3).

(*R*)-MTPAs of (*S*)-2-aza-β-tyrosine methyl ester (8.0 mg) was prepared with (*S*)-(+)-methoxy-trifluoromethylphenylacetic acid chloride and purified in the same way as that of (*S*)-MTPAs of (*S*)-2-aza-β-tyrosine methyl ester. ESI-MS (positive ion) for the $[M + H]^+$ ion at *m*/*z* 629, and HR-ESI-MS (positive ion) for the $[M + H]^+$ ion at *m*/*z* 629.1703 (the calculated $[M + H]^+$ ion for $C_{29}H_{27}F_6N_2O_7$ at *m/z* 629.1717). ^{1}H NMR in $CDCl_3$, δ 2.87 (1H, dd, *J* = 6.5, 16.0 Hz, H-2′a); 3.05 (1H, dd, *J* = 5.6, 16.0 Hz, H-2′b), 3.38 (3H, brs, OMe), 3.58 (3H, s, OMe), 3.68 (3H, brs, OMe), 5.57 (1H, m, H-3′); 7.40-7.64 (12H, overlapped); 8.12 (1H, brd, *J* = 8.7 Hz, NH); 8.40 (1H, d, *J* = 2.4 Hz, H-3).

References

1. Lohman JR, Shen B (2012) 4-Methylideneimidazole-5-one-containing aminomutases in enediyne biosynthesis. *Methods Enzymol* 516:300-319.
2. Christenson SD, Wu W, Spies MA, Shen B, Toney MD (2003) Kinetic analysis of the 4-methylideneimidazole-5-one-containing tyrosine aminomutase in enediyne antitumor antibiotic C-1027 biosynthesis. *Biochemistry* 42:12708-12718.
3. Christianson CV, Montavon TJ, Van Lanen SG, Shen B, Bruner SD (2007) The structure of L-tyrosine 2,3 aminomutase from the C-1027 enediyne antitumor antibiotic biosynthetic pathway. *Biochemistry* 46:7205-7214.
4. Cooke HA, Bruner SD (2010) Probing the active site of MIO-dependent aminomutases, key catalysts in the biosynthesis of beta-amino acids incorporated in secondary metabolites. *Biopolymers* 93:802-810.
5. Lohman JR, Huang S-X, Horsman GP, Dilfer PE, Huang T, Chen Y, Wendt-Pienkowski E, Shen B (2013) Cloning and sequencing of the kedarcidin biosynthetic gene cluster from *Streptoalloteichus* sp. ATCC 53650 revealing new insights into biosynthesis of the enediyne family of antitumor antibiotics. *Mol BioSyst* 9:478-489.
6. Inouye S, Shomura T, Tsuruoka T, Ogawa Y, Watanabe H, Yoshida J, Niida T (1975) L-*β*-(5-hydroxy-2-pyridyl)-alanine and L-*β*-(3-hydroxyureido)-alanine from *Streptomyces*. *Chem Pharm Bull* 23:2669-2677.
7. Dale JA, Mosher HS (1973) Nuclear magnetic resonance enantiomer regents. Configurational correlations via nuclear magnetic resonance chemical shifts of diastereomeric mandelate, O-methylmandelate, and α-methoxy-α-trifluoromethylphenylacetate (MTPA) esters. *J Am Chem Soc* 95:512-519.
8. Seco JM, Quiñoá E, Riguera R (2001) A practical guide for the assignment of the absolute configuration of alcohols, amines and carboxylic acids by NMR. *Tetrahedron Asymmetry* 12:2915-2925.
9. Adamczyk M, Reddy RE (2001) Synthesis of (*R*)-(+)-methyl 3-amino-3-(5-hydroxy-2-pyridinyl)propanoate, an analog of L-azatyrosine. *Tetrahedron Asymmetry* 12:1047-1054.

Figure S1. MIO-containing ammonia lyases, aminomutases, and KedY4. (*A*) Post-translational formation of the MIO-prosthetic group from the conserved Ala-Ser-Gly motif. (*B*) Proposed mechanisms of MIO-containing ammonia lyases (path a) and aminomutase (path b). (*C*) Sequence alignments of KedY4 with other functionally characterized aminomutases, supporting its functional annotation as an MIO-containing aminomutase. Residue numbering is corresponding to SgcC4. The highly conserved ASG motif for the MIO-prosthetic group, as well as other active site residues, are marked in blue. The residues that are directly involved L-tyrosine specificity in TAMs are marked in red.

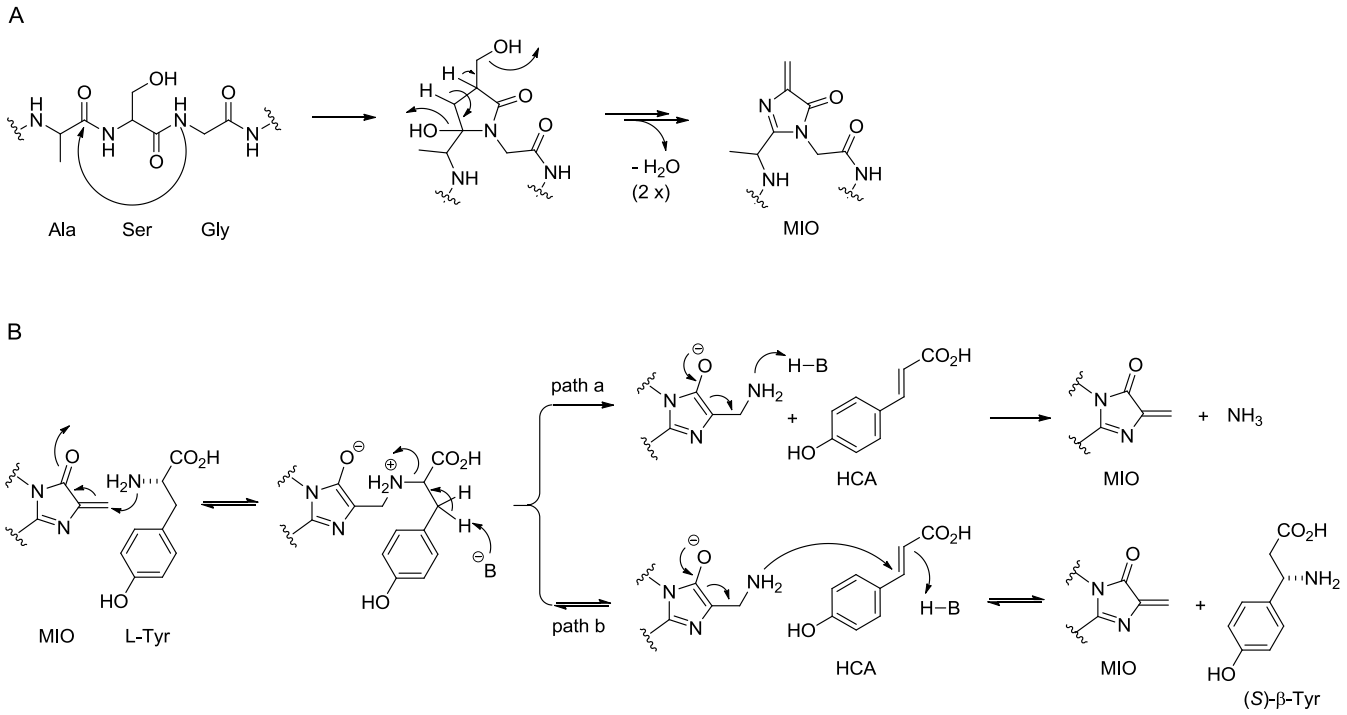

C

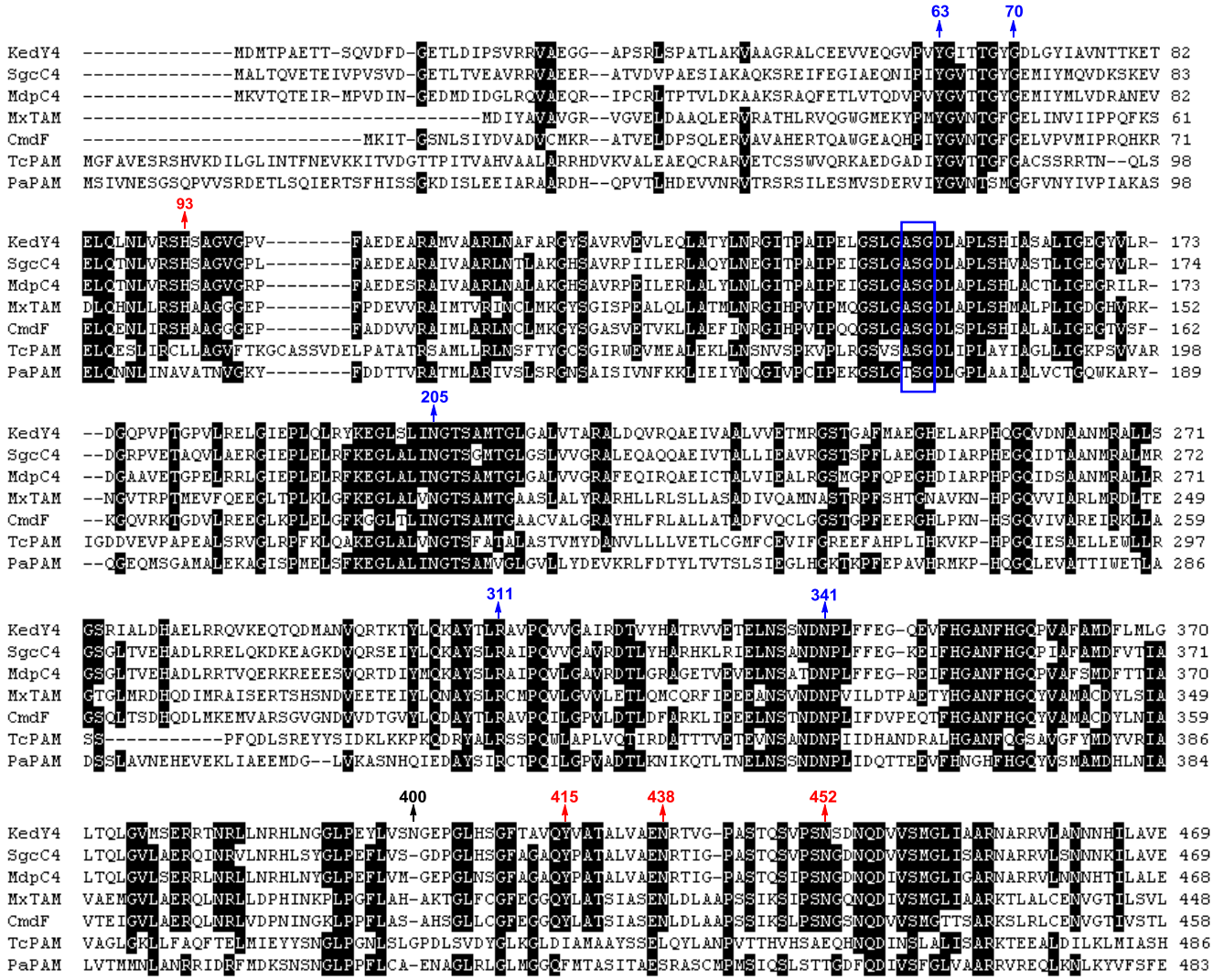
63
70
93
205
311
341
400
415
438
452
KedY4
SgcC4
MdpC4
MxTAM
CmdF
TcPAM
PaPAM

Figure S2. Purification of KedY4. (*A*) SDS-PAGE of the purified KedY4: lane 1, His_6-tagged-KedY4 and lane 2, protein MW standards. (*B*) UV absorption spectrum of the KedY4 protein whose His_6-tag was removed upon TEV treatment.

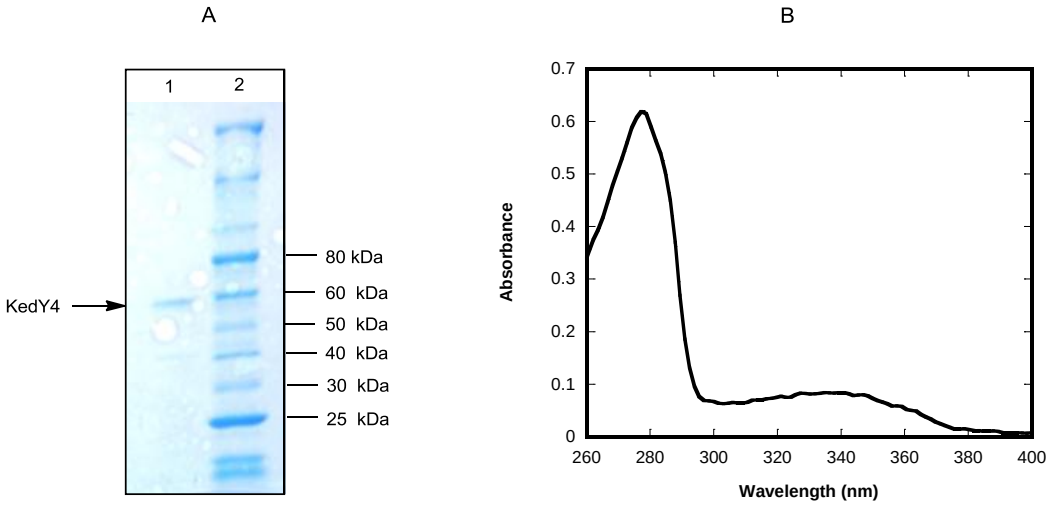

Figure S3. ^{1}H NMR spectrum of 2-aza-L-tyrosine, isolated from *S. chibaensis* SF-1346, in D_2O

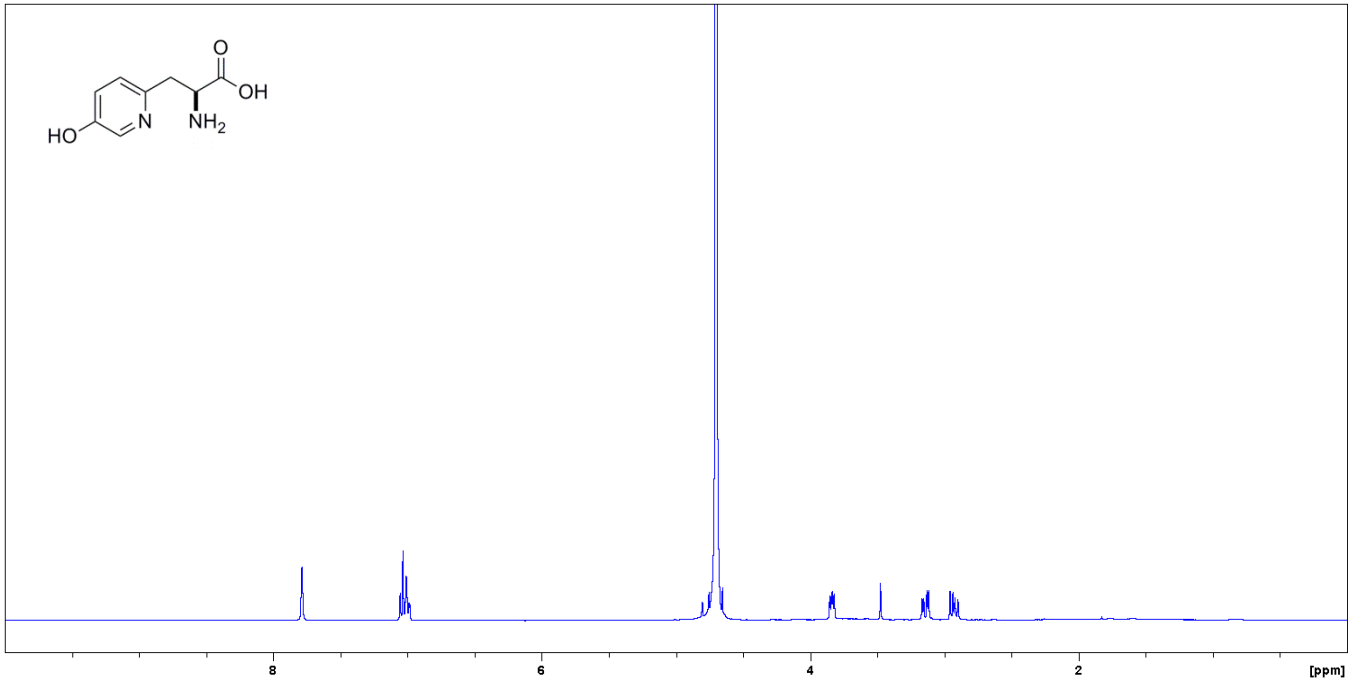

Figure S4. ^{13}C NMR spectrum of 2-aza-L-tyrosine, isolated from *S. chibaensis* SF-1346, in D_2O

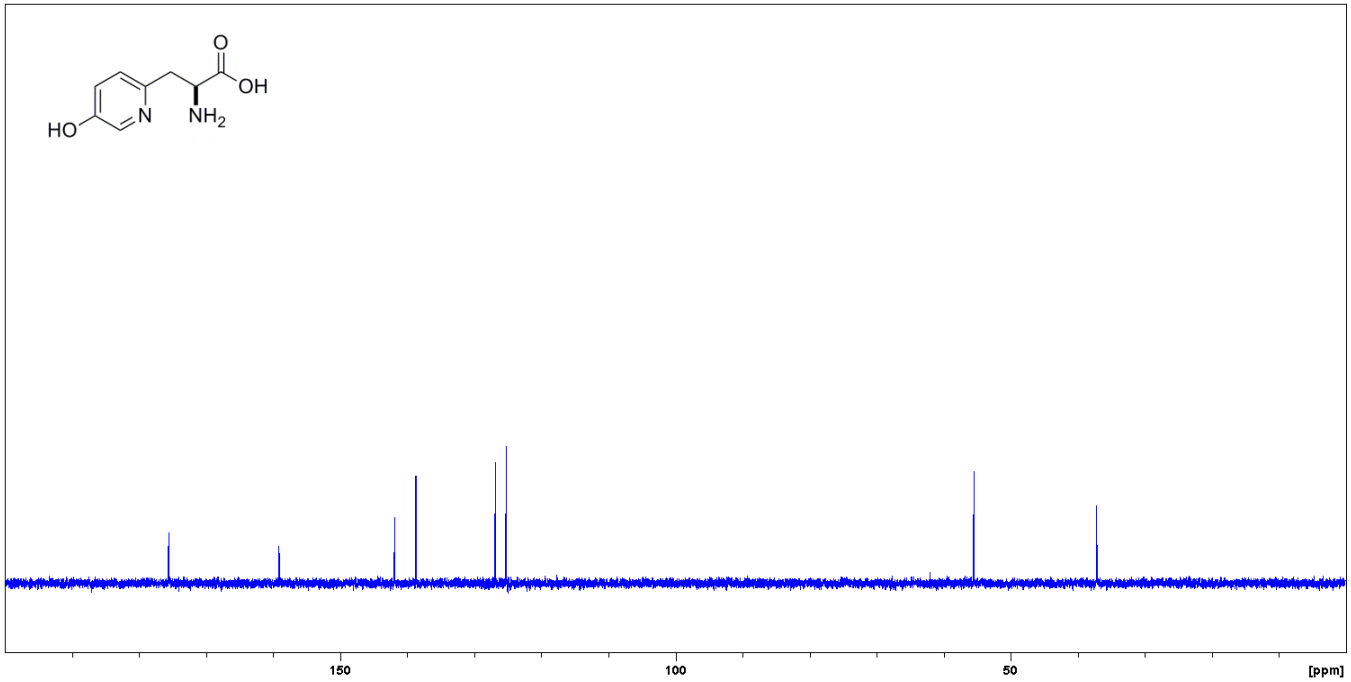

Figure S5. Chemical synthesis of (*A*) (*R*)- and (*S*)-2-aza-β-tyrosine and their methyl esters from 5-hydroxy-2-methylpyridine and (*B*) conversion of (*R*)- and (*S*)-2-aza-β-tyrosine methyl esters into their (*R*)- and (*S*)-MTPAs.

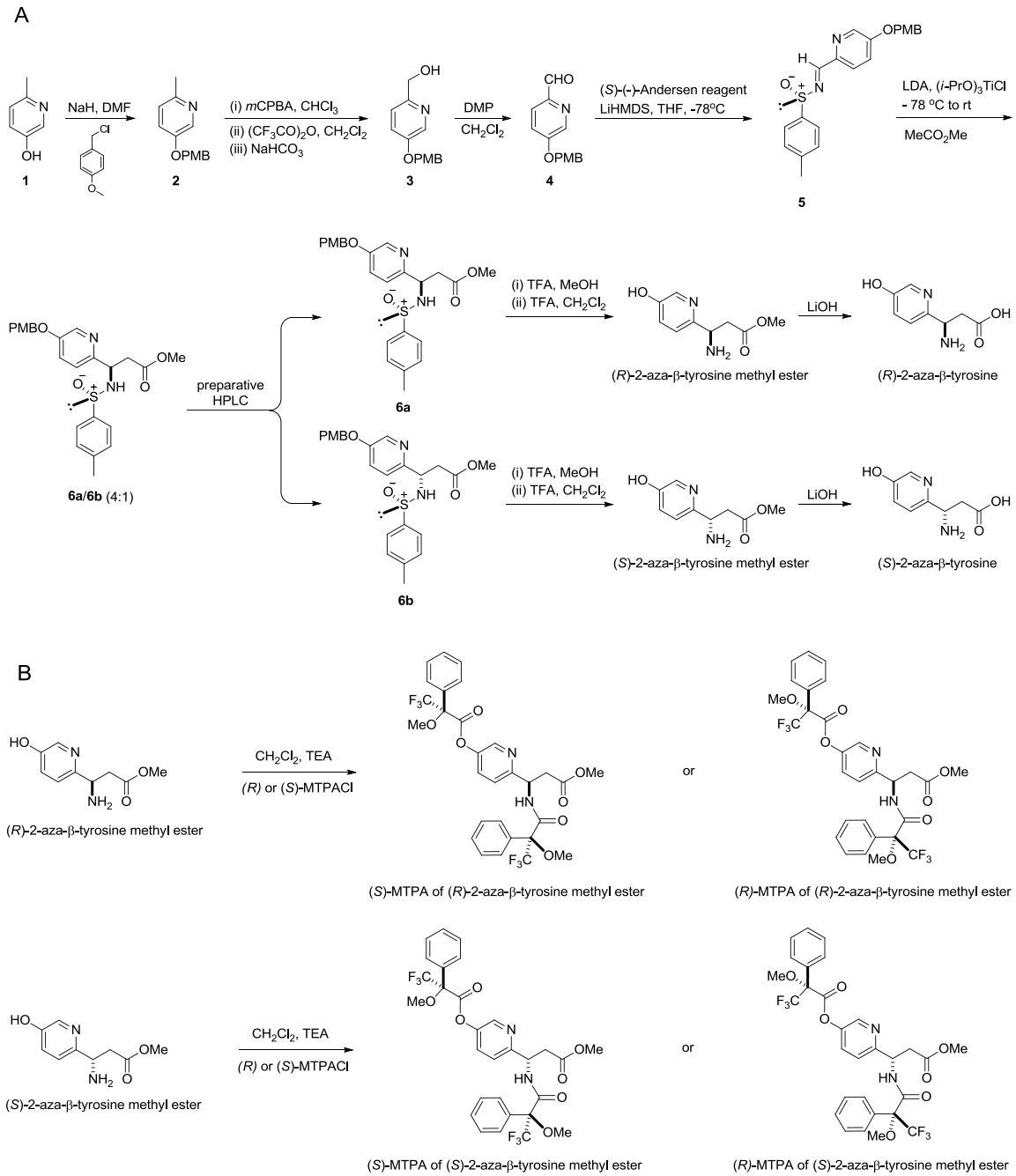

Figure S6. ^{1}H NMR spectrum of intermediate **2** for (*R*)- and (*S*)-2-aza-β-tyrosine synthesis in $CDCl_3$

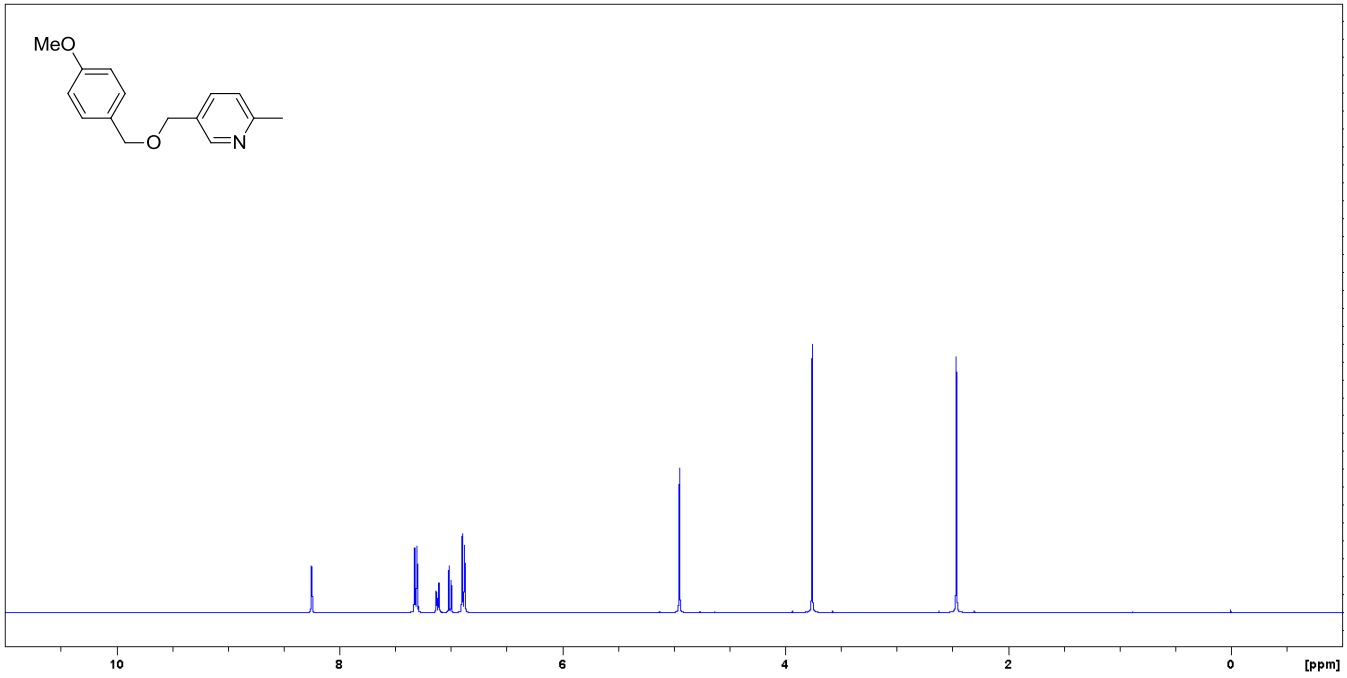

Figure S7. ^{13}C NMR spectrum of intermediate **2** for (*R*)- and (*S*)-2-aza-β-tyrosine synthesis in $CDCl_3$

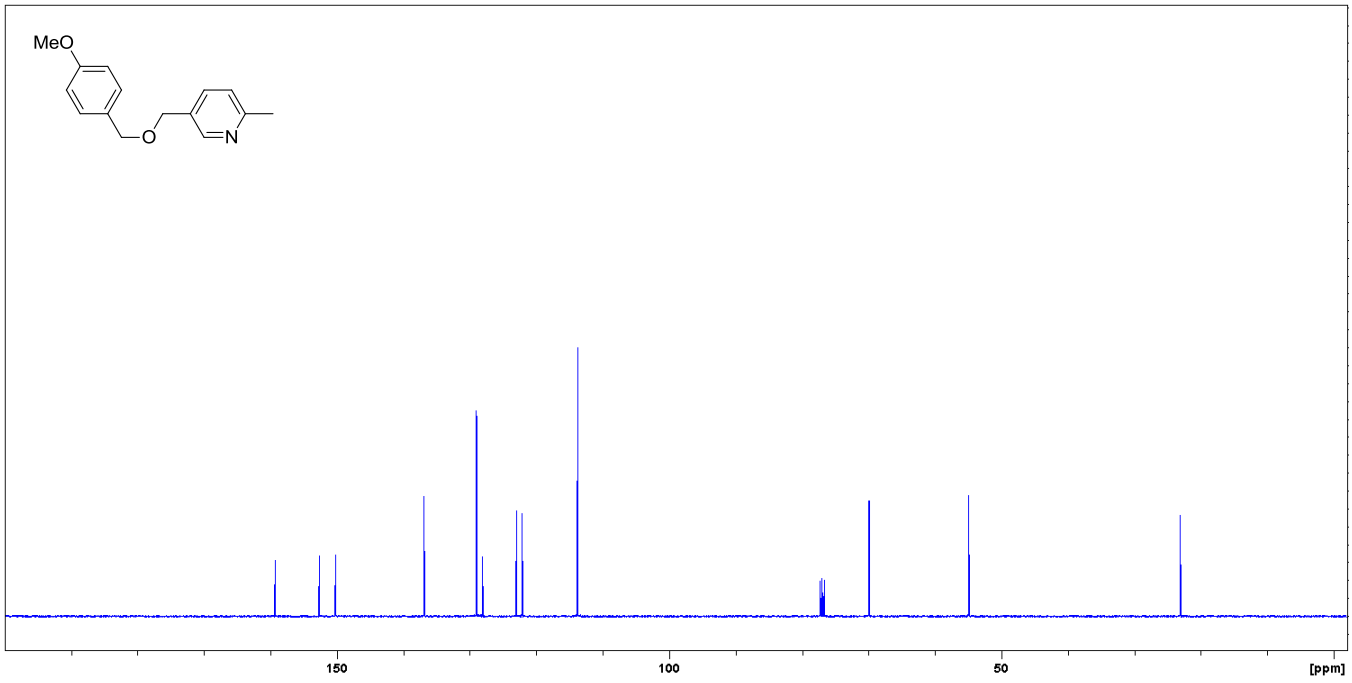

Figure S8. ^{1}H NMR spectrum of intermediate **3** for (*R*)- and (*S*)-2-aza-β-tyrosine synthesis in $CDCl_3$

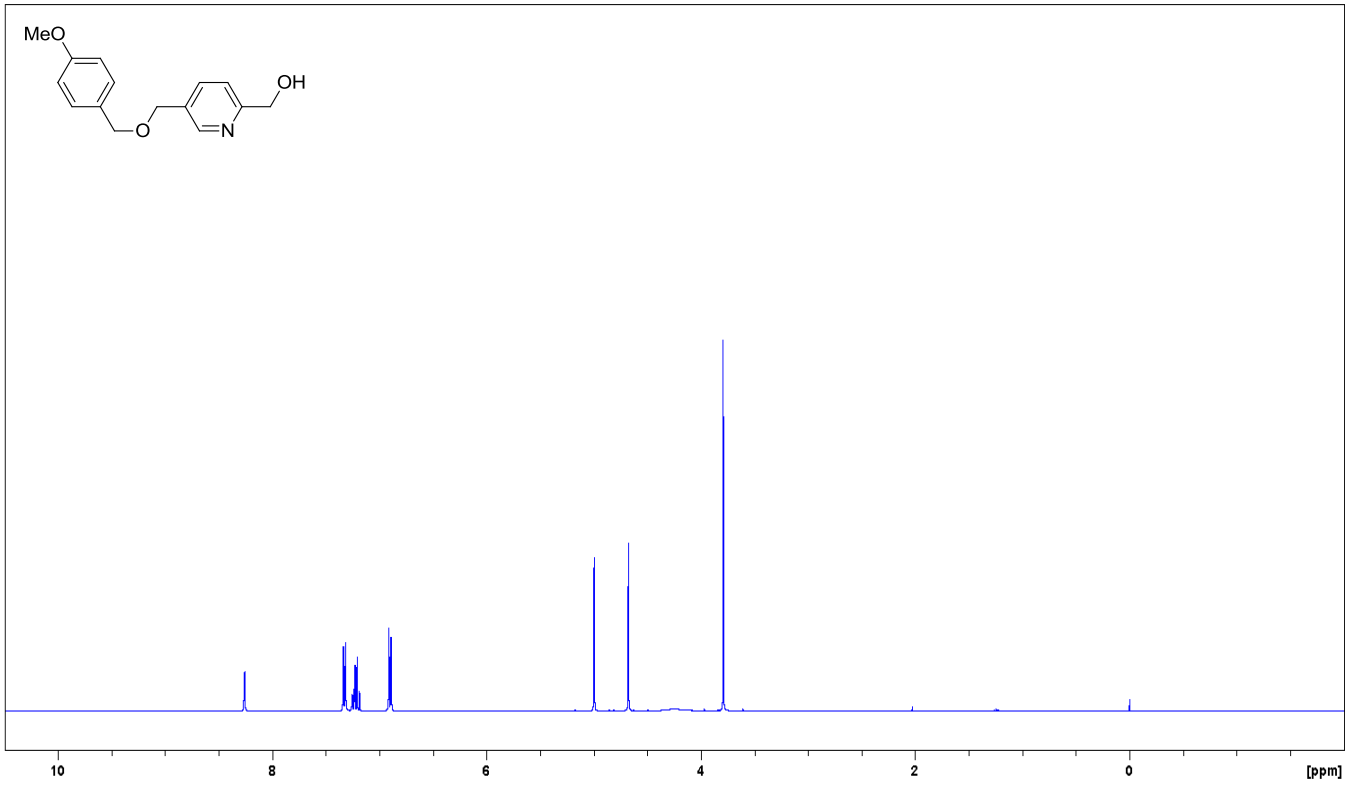

Figure S9. ^{13}C NMR spectrum of intermediate **3** for (*R*)- and (*S*)-2-aza-β-tyrosine synthesis in $CDCl_3$

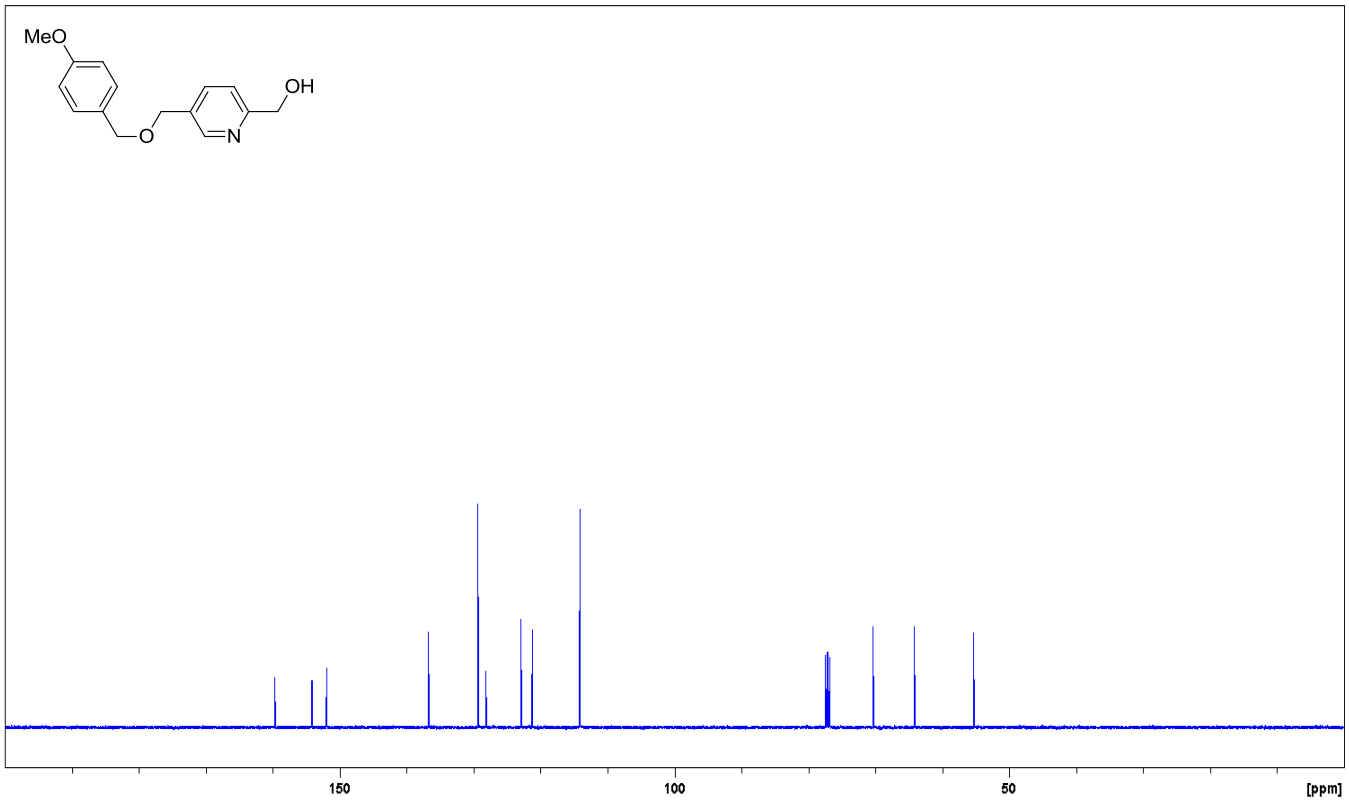

Figure S10. ^{1}H NMR spectrum of intermediate **4** for (*R*)- and (*S*)-2-aza-β-tyrosine synthesis in $CDCl_3$

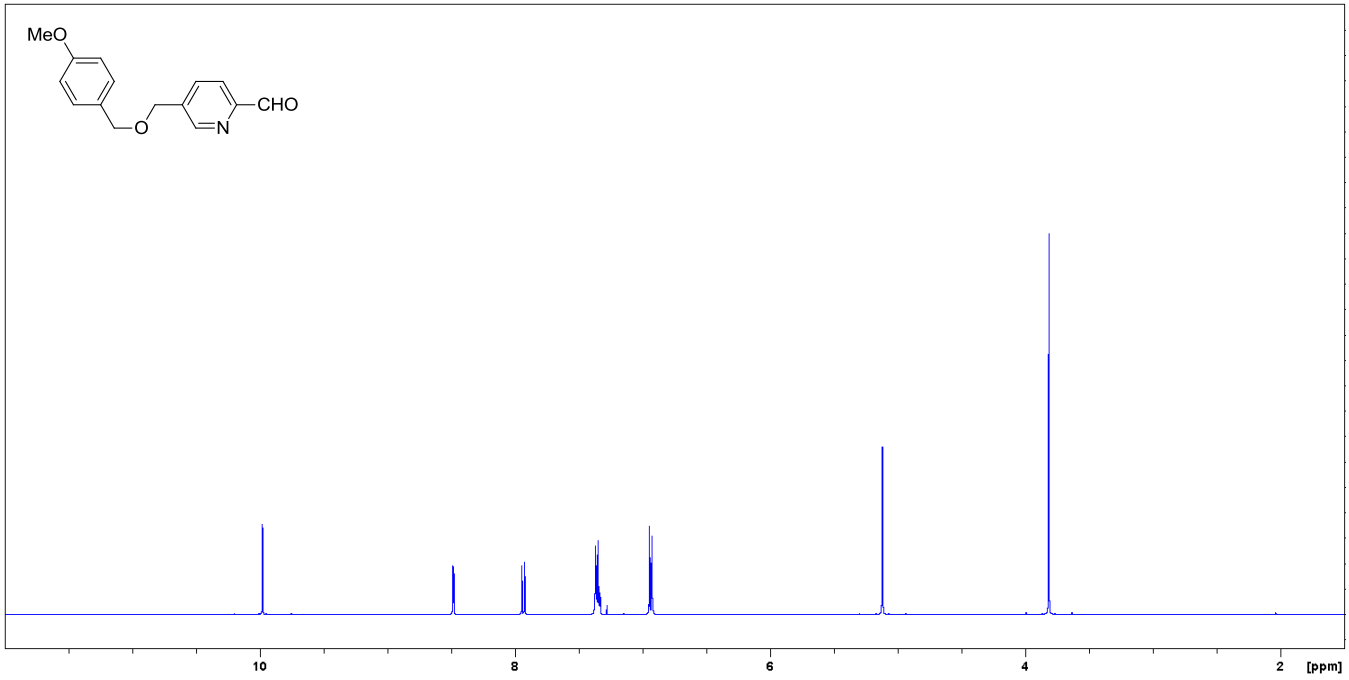

Figure S11. ^{13}C NMR spectrum of intermediate **4** for (*R*)- and (*S*)-2-aza-β-tyrosine synthesis in $CDCl_3$

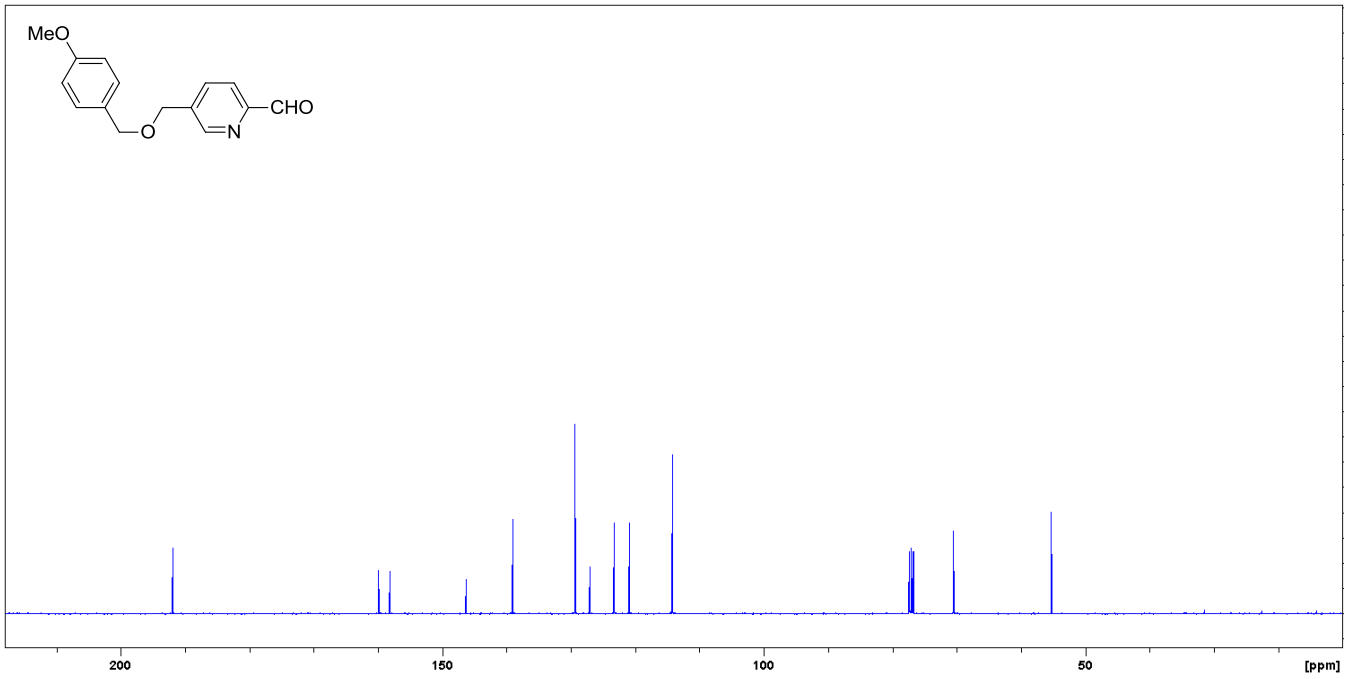

Figure S12. ^{1}H NMR spectrum of intermediate **5** for (*R*)- and (*S*)-2-aza-β-tyrosine synthesis in $CDCl_3$

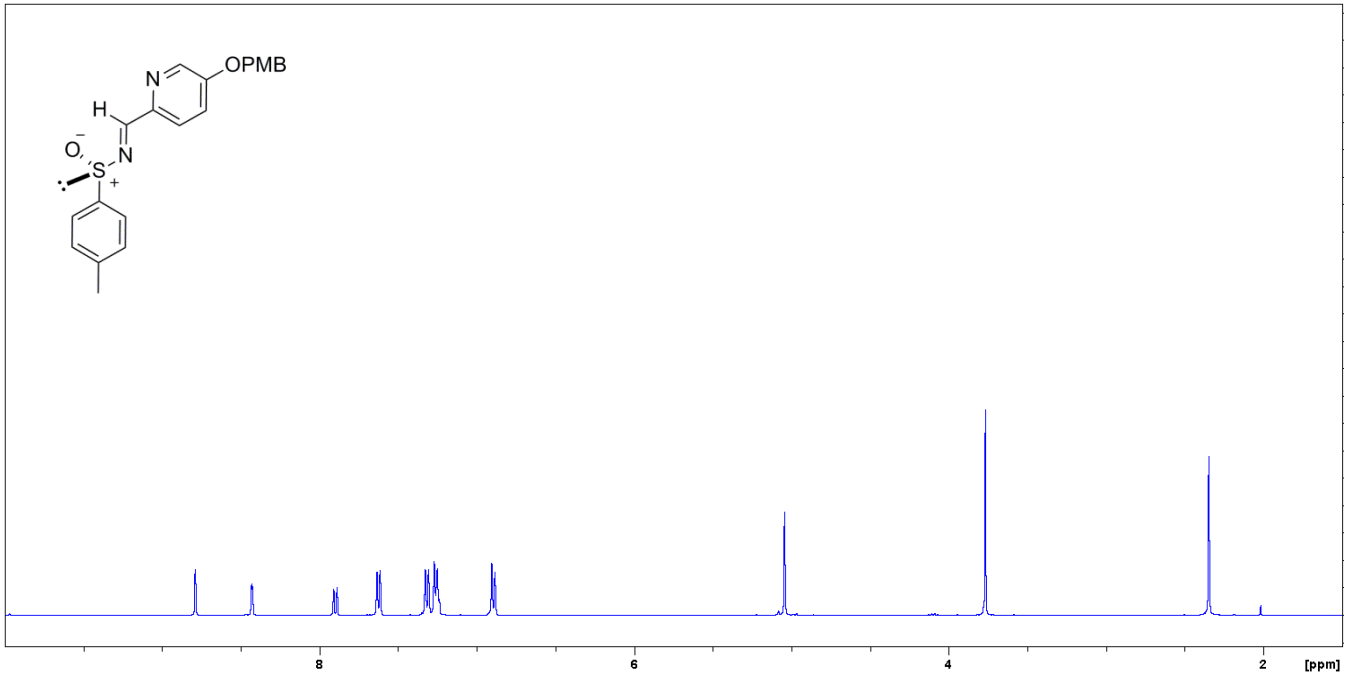

Figure S13. ^{13}C NMR spectrum of intermediate **5** for (*R*)- and (*S*)-2-aza-β-tyrosine synthesis in $CDCl_3$

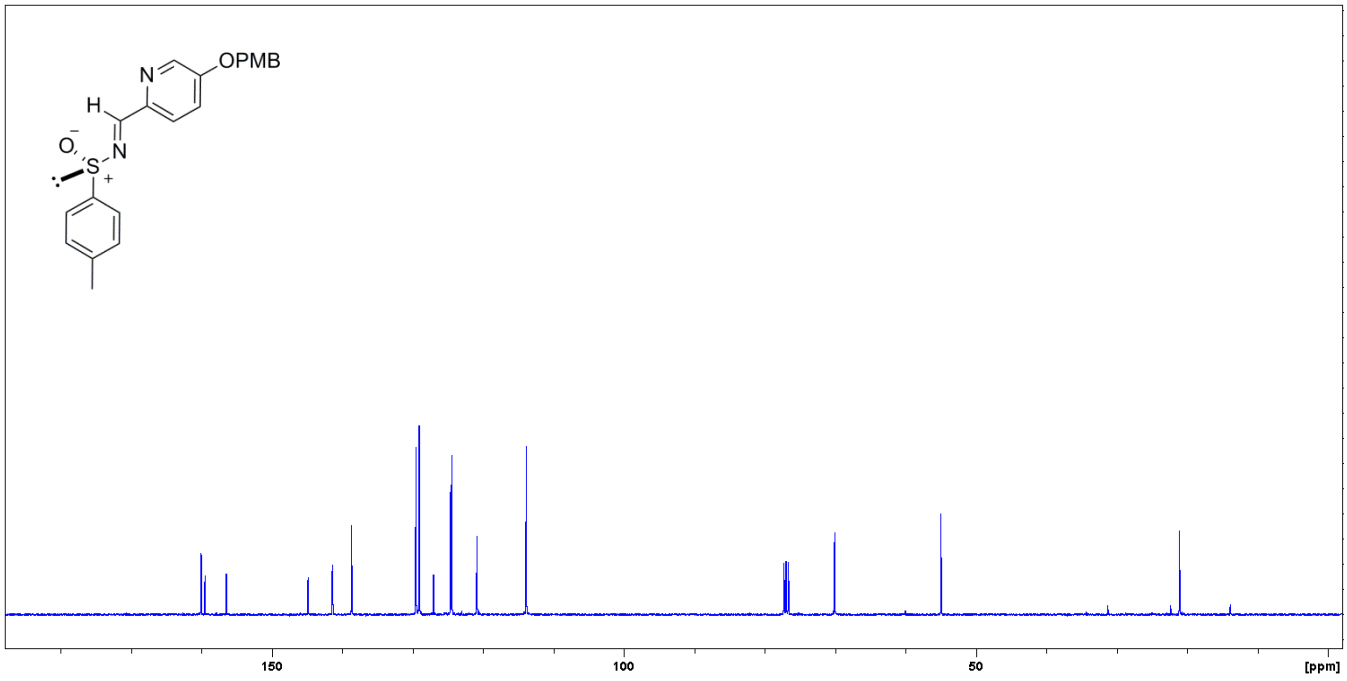

Figure S14. ^{1}H NMR spectrum of intermediate **6a** for (*R*)-2-aza-β-tyrosine synthesis in $CDCl_3$

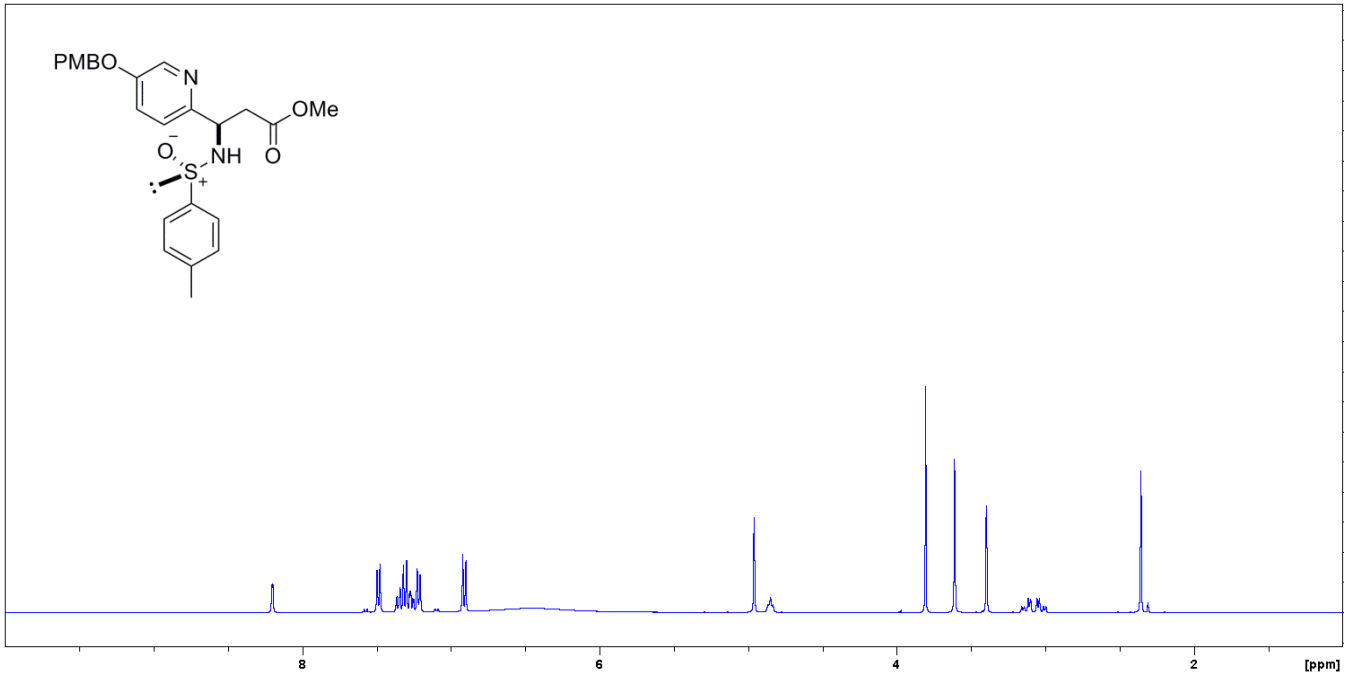

Figure S15. ^{13}C NMR spectrum of intermediate **6a** for (*R*)-2-aza-β-tyrosine synthesis in $CDCl_3$

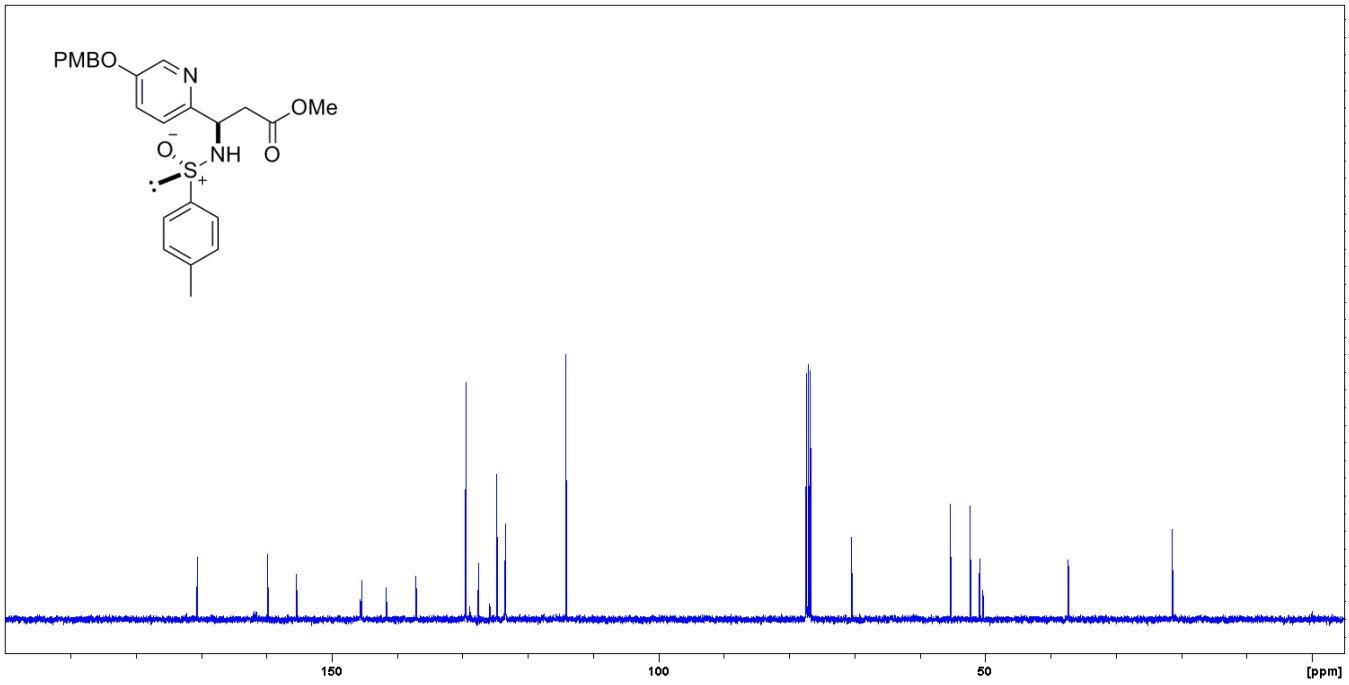

Figure S16. ^{1}H NMR spectrum of intermediate **6b** for (*S*)-2-aza-β-tyrosine synthesis in $CDCl_3$

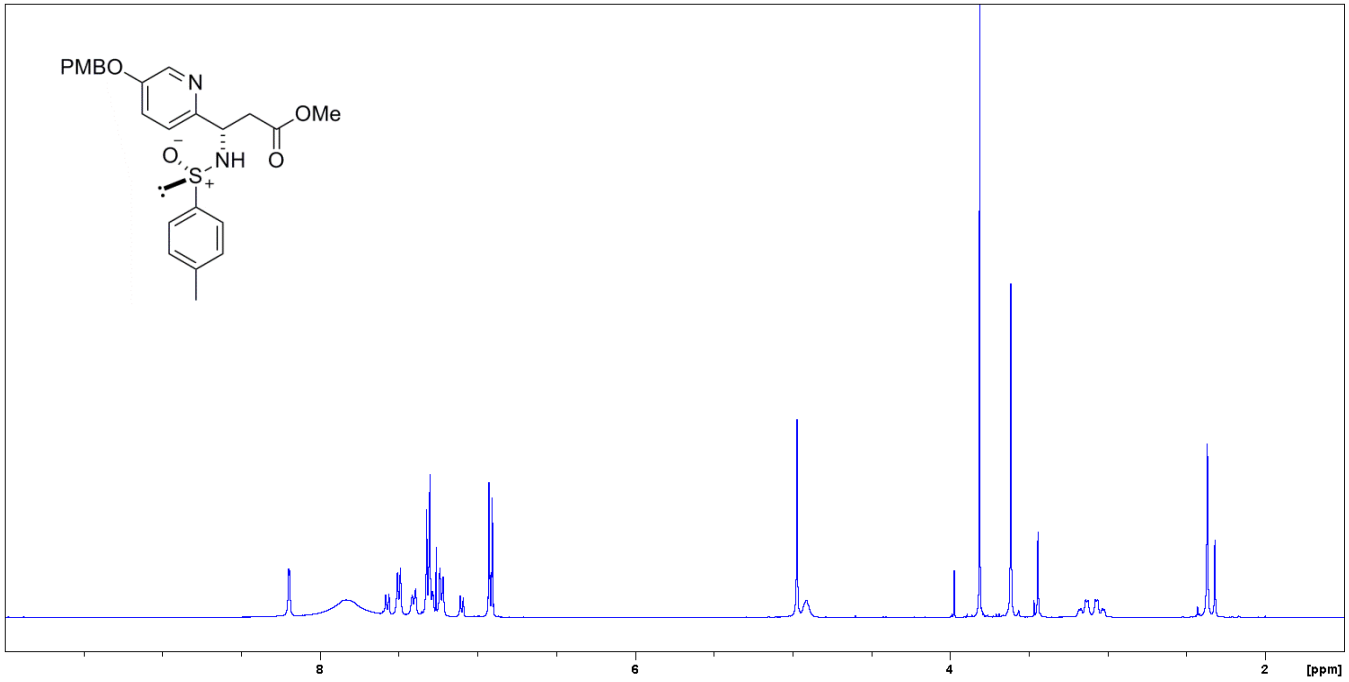

Figure S17. ^{13}C NMR spectrum of intermediate **6b** for (*S*)-2-aza-β-tyrosine synthesis in $CDCl_3$

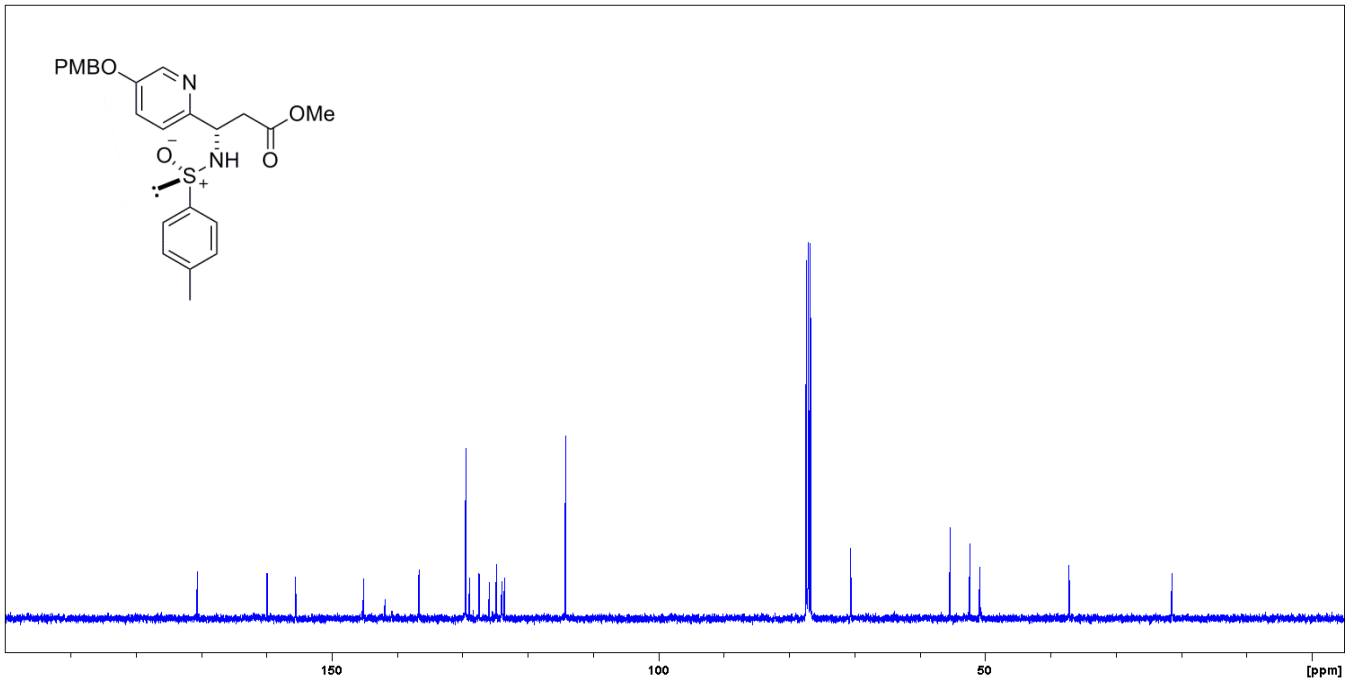

Figure S18. ^{1}H NMR spectrum of chemically synthesized (*R*)-2-aza-β-tyrosine methyl ester in CD_3OD

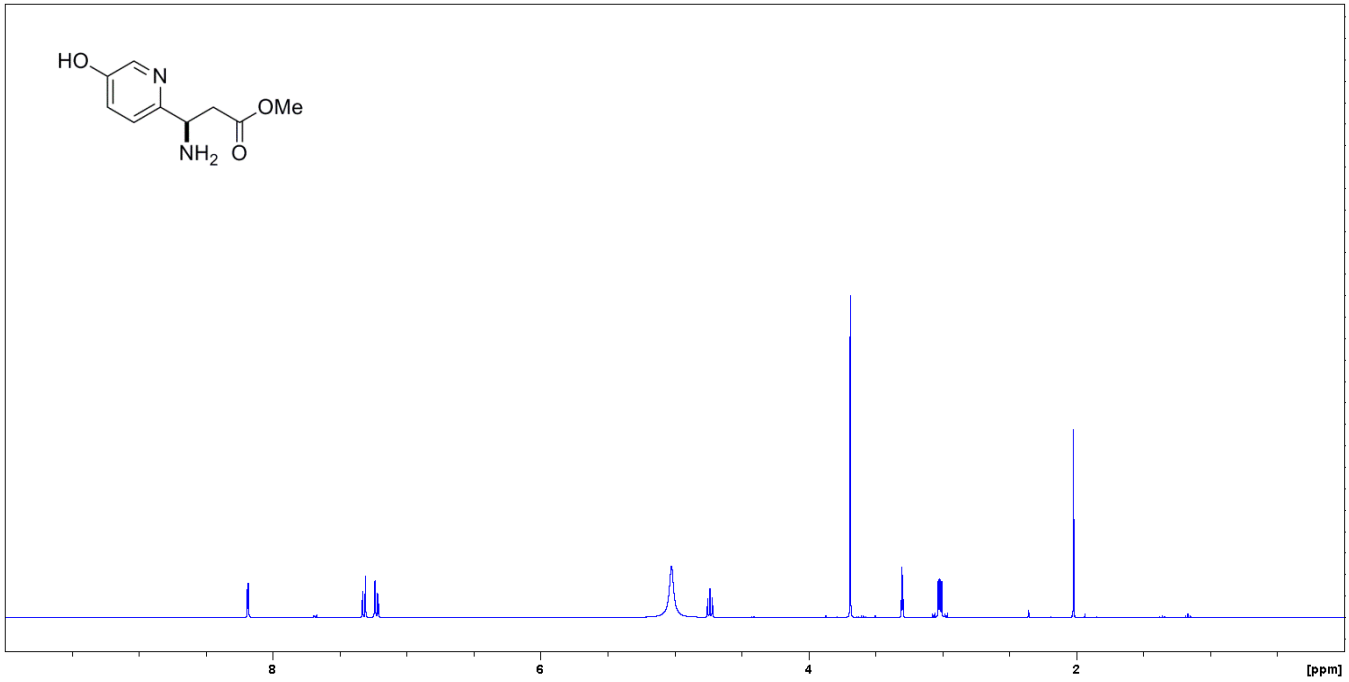

Figure S19. ^{13}C NMR spectrum of chemically synthesized (*R*)-2-aza-β-tyrosine methyl ester in CD_3OD

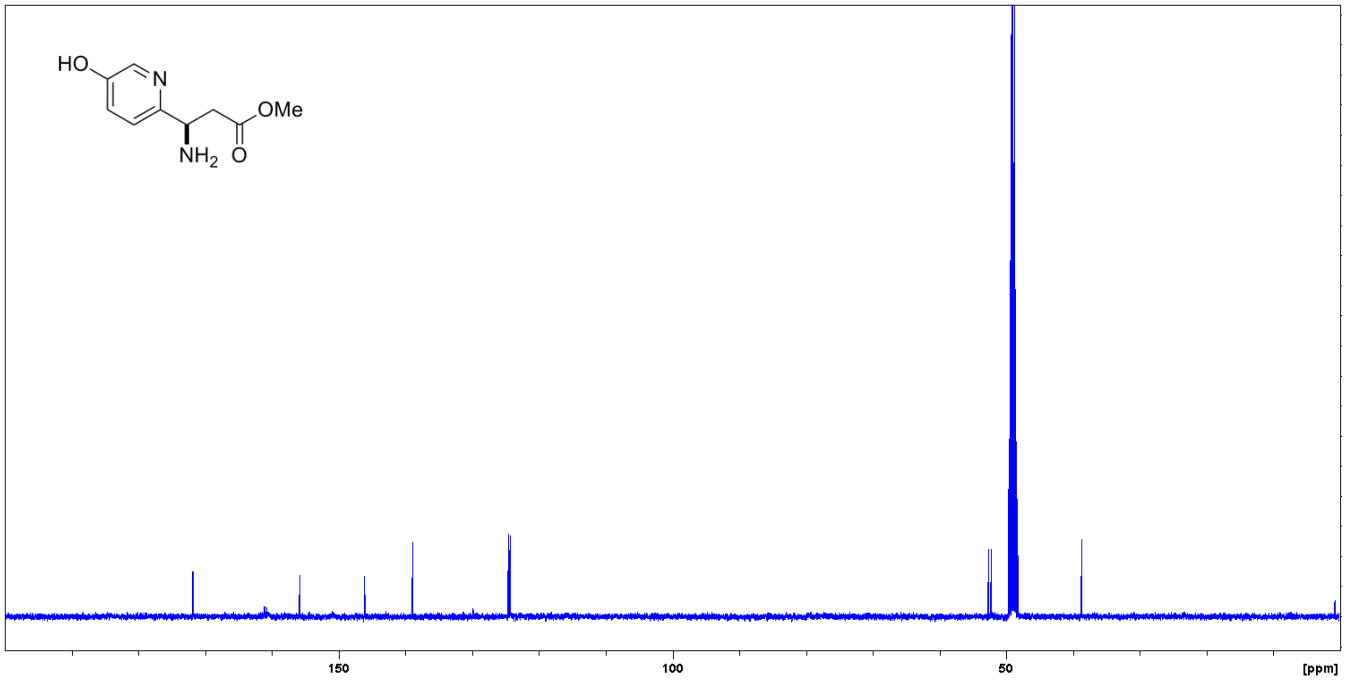

Figure S20. ^{1}H NMR spectrum of chemically synthesized (*R*)-2-aza-β-tyrosine in D_2O

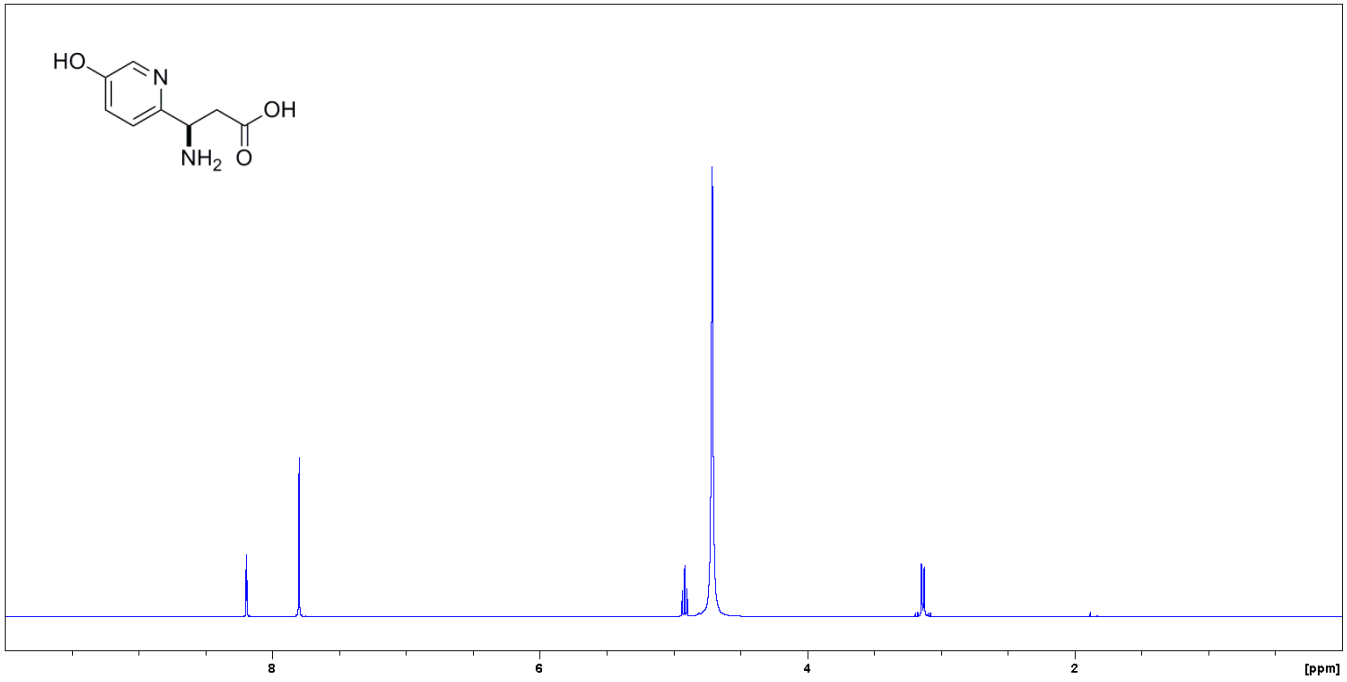

Figure S21. ^{13}C NMR spectrum of chemically synthesized (*R*)-2-aza-β-tyrosine in D_2O

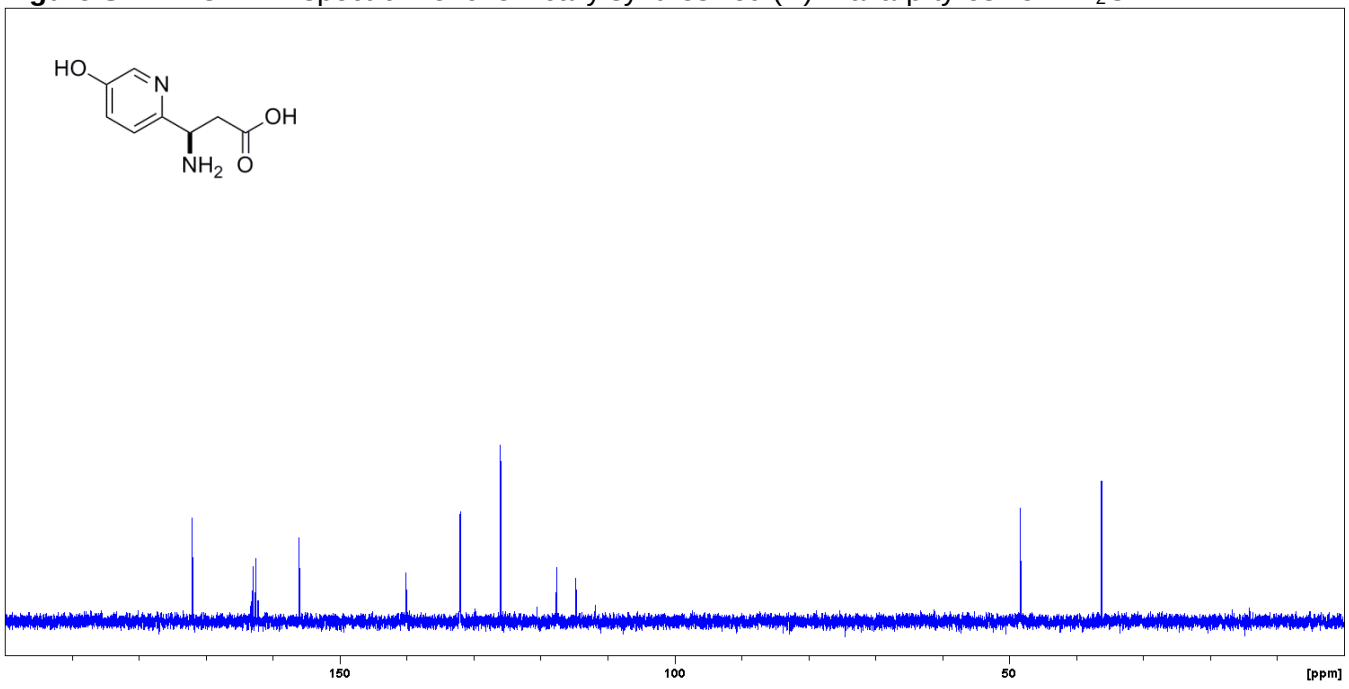

Figure S22. HSQC NMR spectrum of chemically synthesized (*R*)-2-aza-β-tyrosine in D_2O

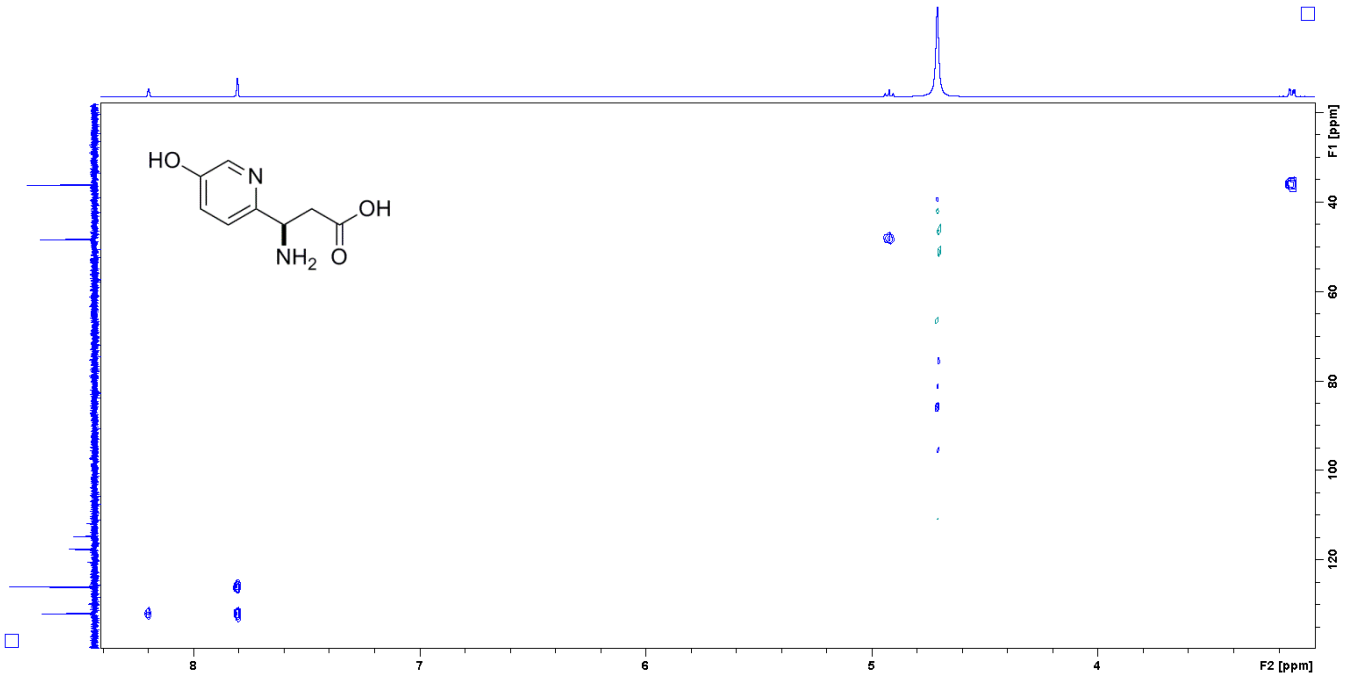

Figure S23. HMBC NMR spectrum of chemically synthesized (*R*)-2-aza-β-tyrosine in D_2O

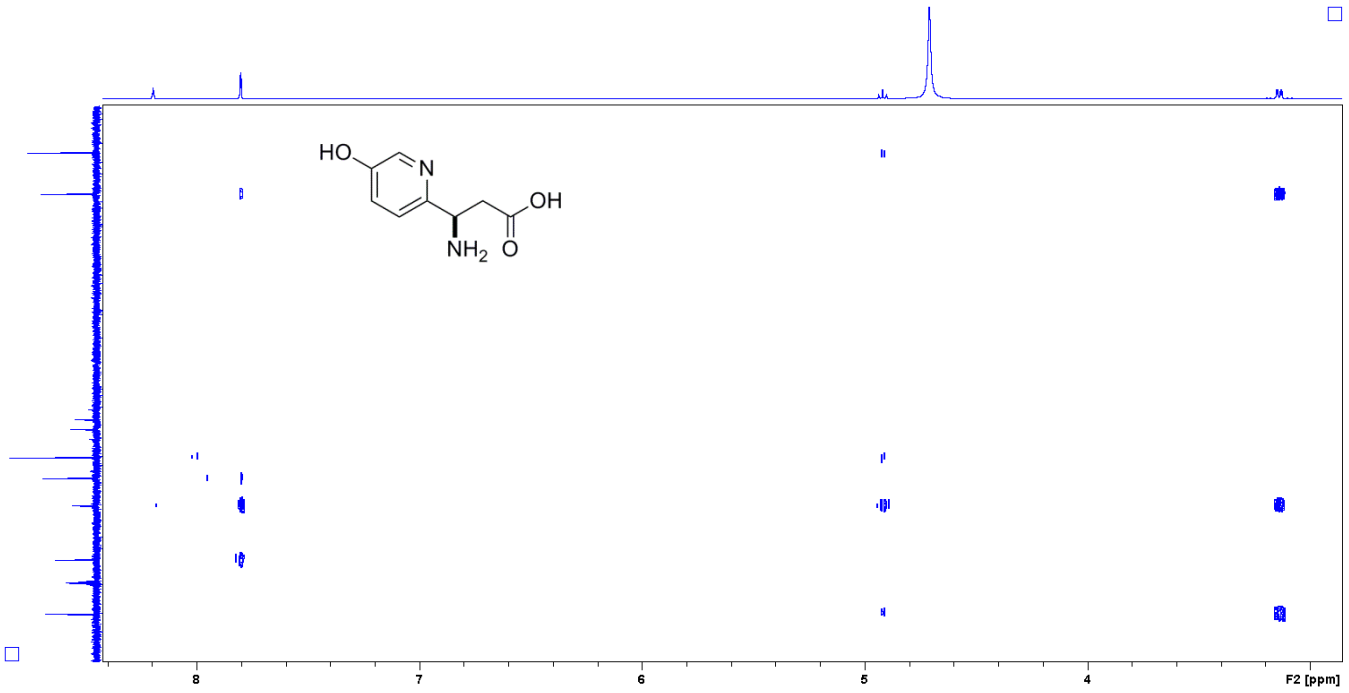

Figure S24. The effect of pH on the initial rate of KedY4-catalyzed formation of (*R*)-2-aza-β-tyrosine (♦) and 2-aza-4-hydroxycinnamic acid (○) from 2-aza-L-tyrosine.

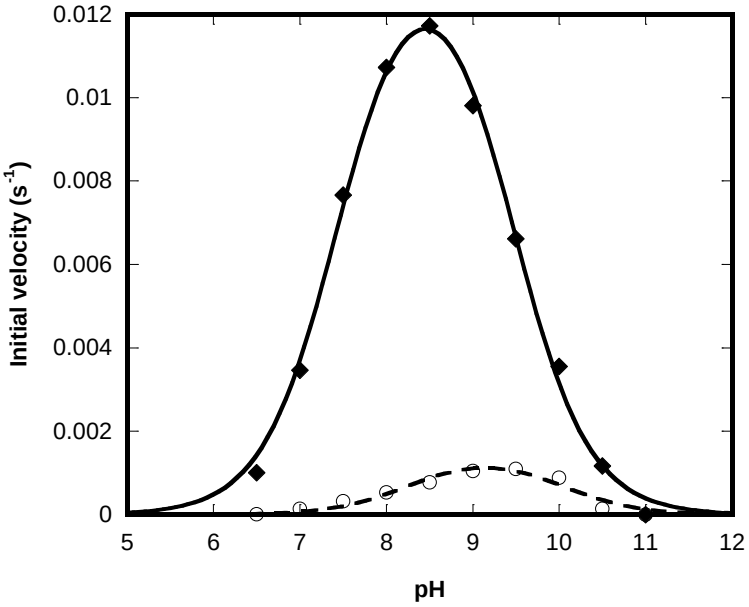

Figure S25. (*A*) SgcC4-catalyzed synthesis of (*R*)-2-aza-β-tyrosine and 2-aza-4-hydroxycinnamic acid from 2-aza-L-tyrosine and conversion of enzymatically synthesized (*R*)-2-aza-β-tyrosine into (*R*)-2-aza-β-tyrosine methyl ester and its (*R*)- and (S)-MTPAs. (*B*) Selected HMBC and COSY correlations supporting the structural assignment of enzymatically synthesized (*R*)-2-aza-β-tyrosine.

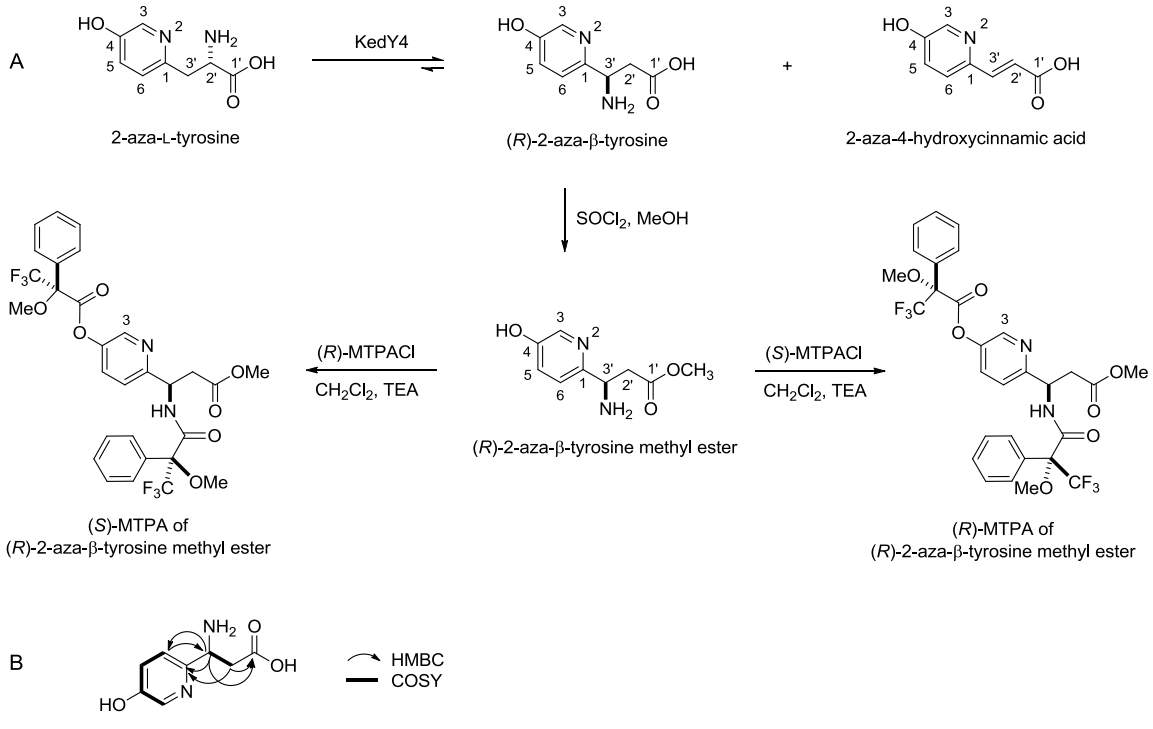

Figure S26. ^{1}H NMR spectrum of enzymatically synthesized (*R*)-2-aza-β-tyrosine as a BTP complex in D_2O.

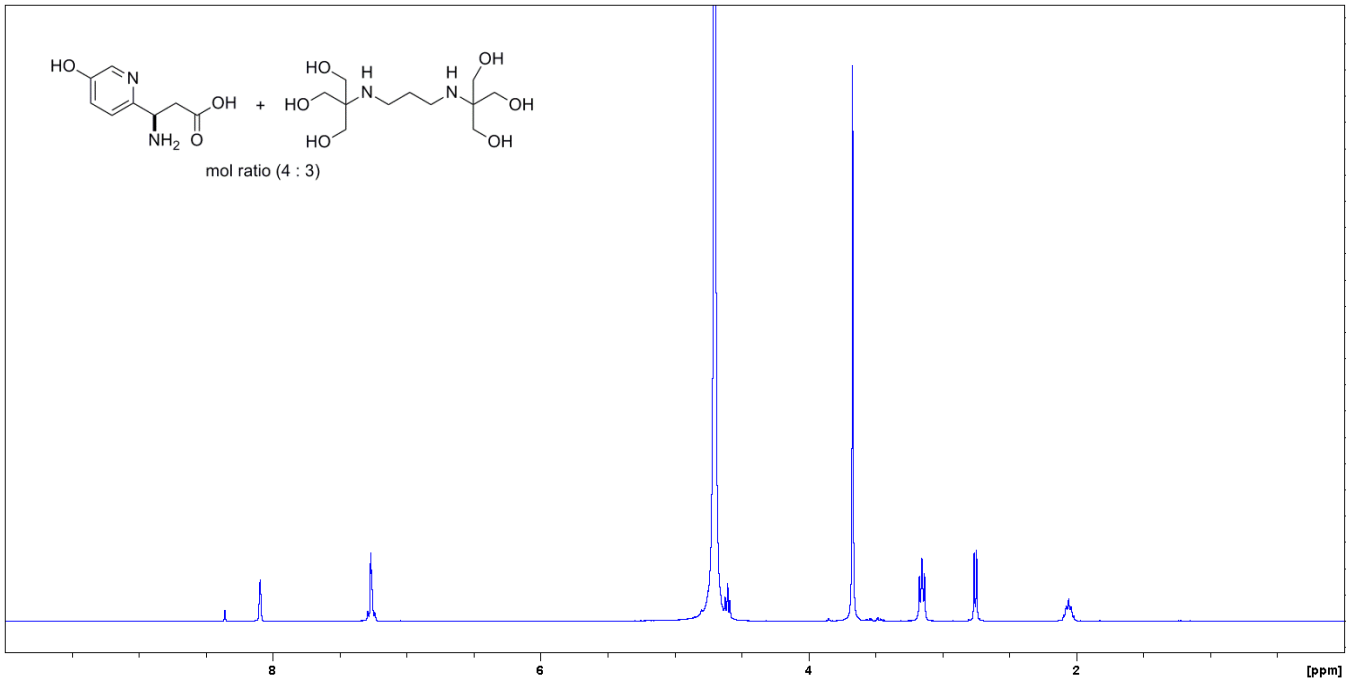

Figure S27. ^{13}C NMR spectrum of enzymatically synthesized (*R*)-2-aza-β-tyrosine as a BTP complex in D_2O.

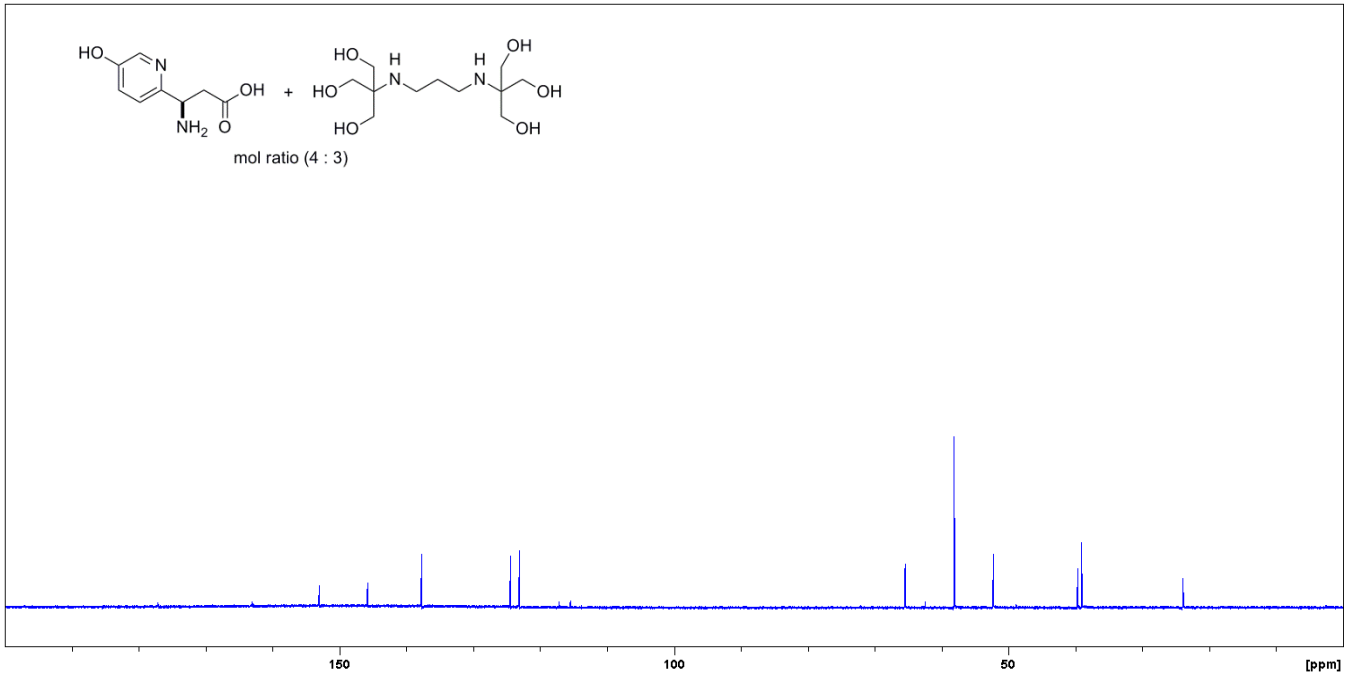

Figure S28. COSY NMR spectrum of enzymatically synthesized (*R*)-2-aza-β-tyrosine as a BTP complex in D_2O.

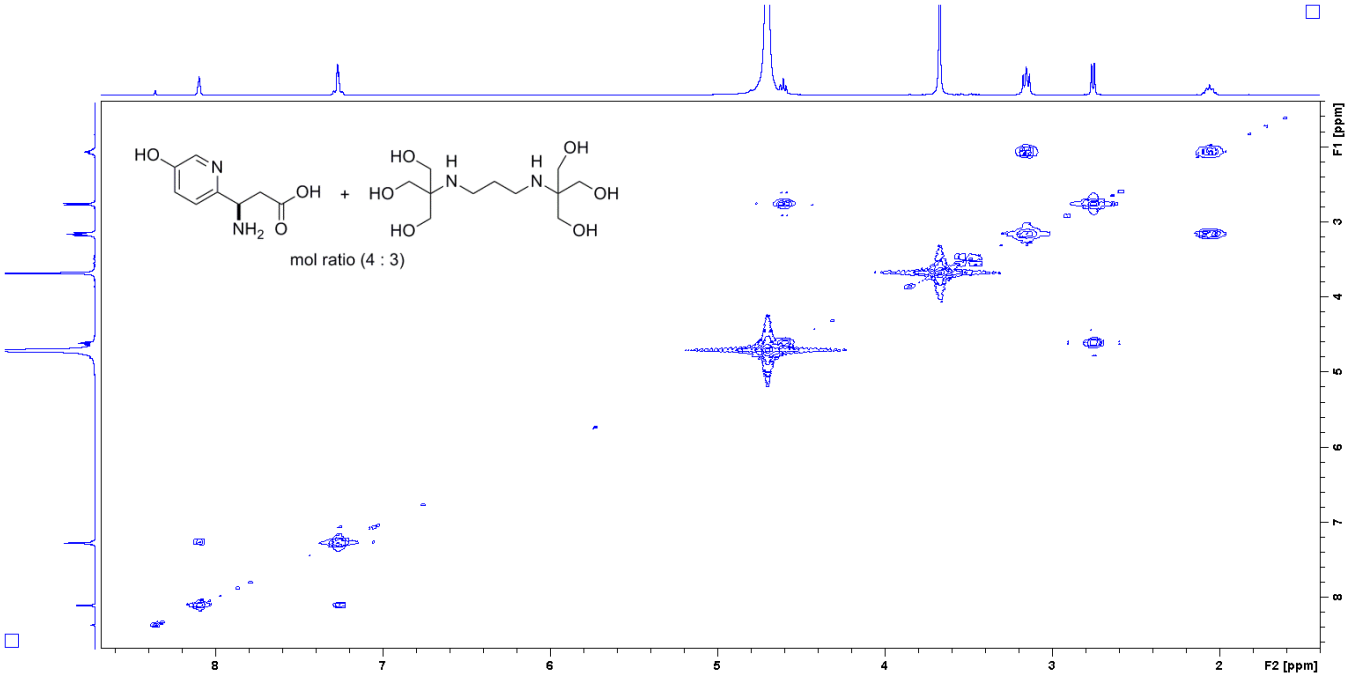

Figure S29. HSQC NMR spectrum of enzymatically synthesized (*R*)-2-aza-β-tyrosine as a BTP complex in D_2O.

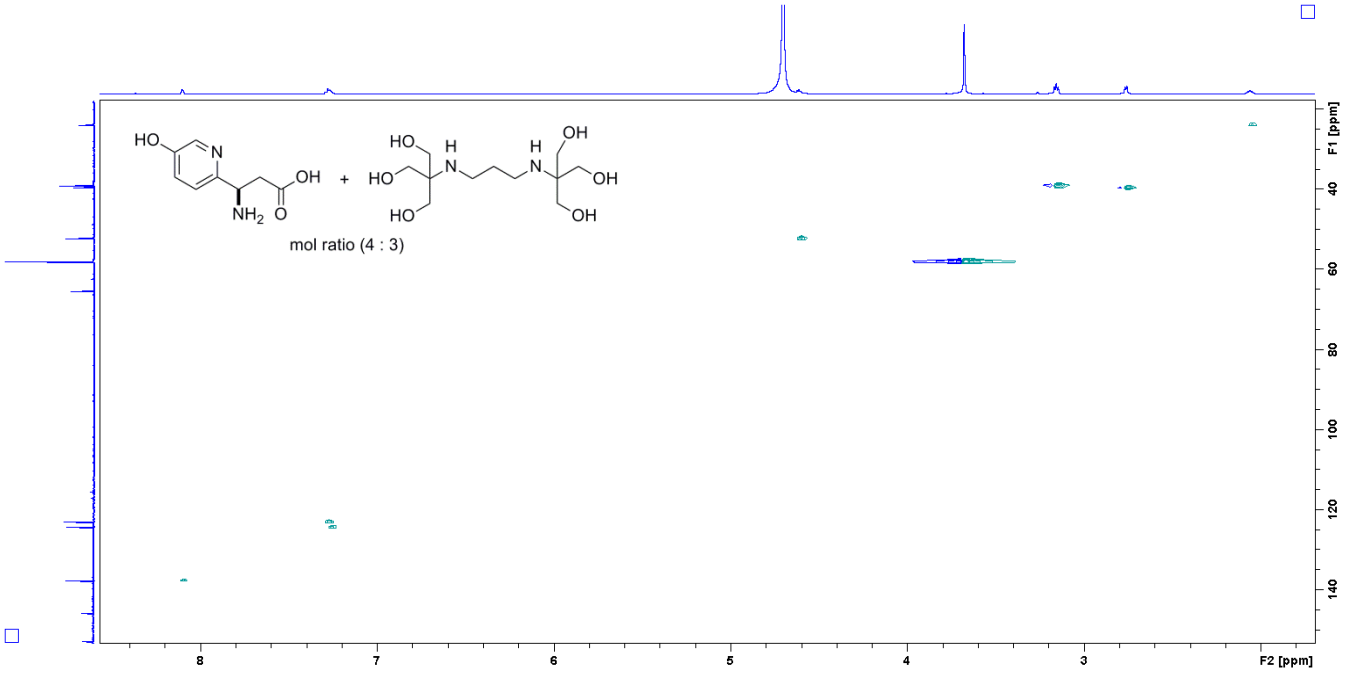

Figure S30. HMBC NMR spectrum of enzymatically synthesized (*R*)-2-aza-β-tyrosine as a BTP complex in D_2O.

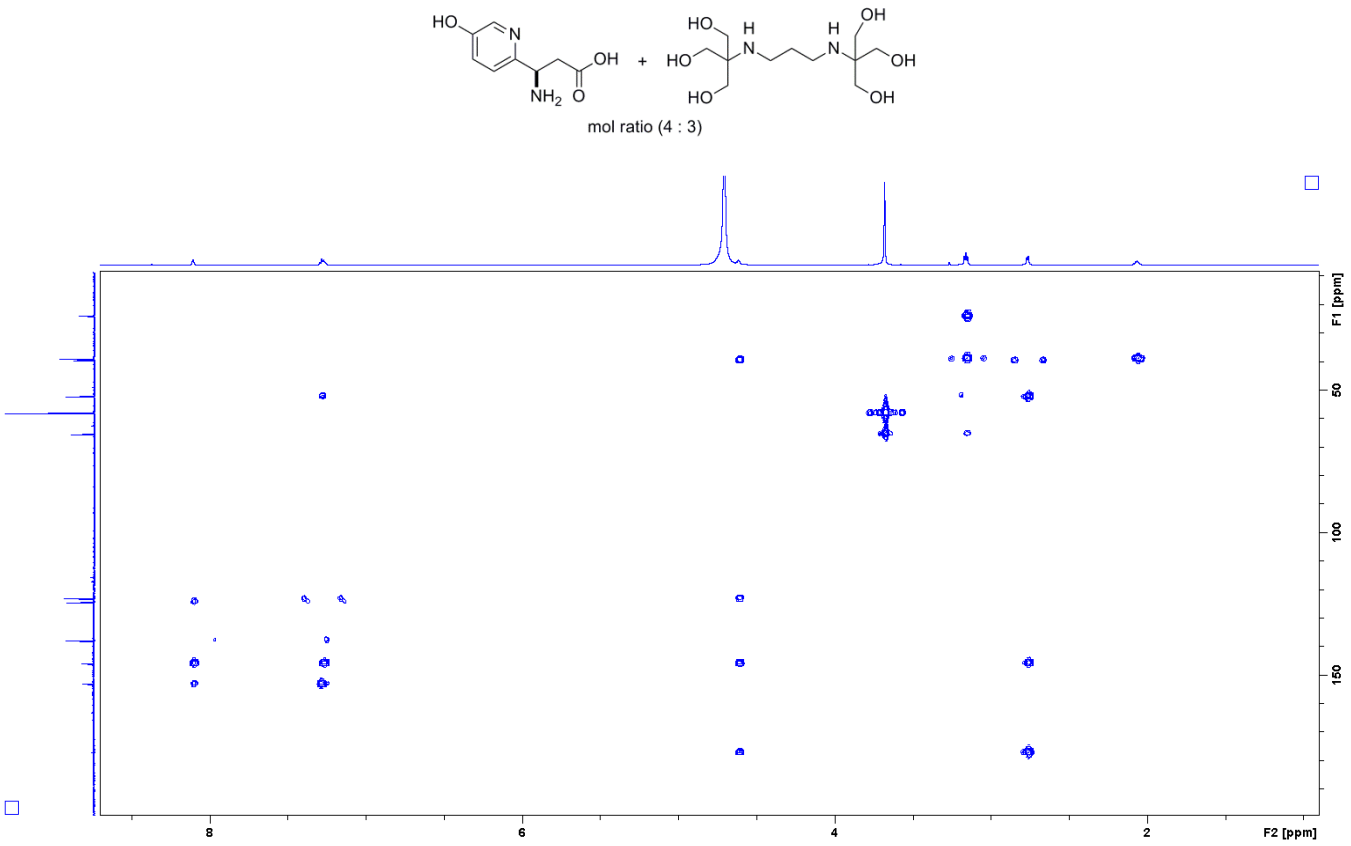

Figure S31. ^{1}H NMR spectrum of enzymatically synthesized 2-aza-4-hydroxycinnamic acid as a BTP complex in D_2O.

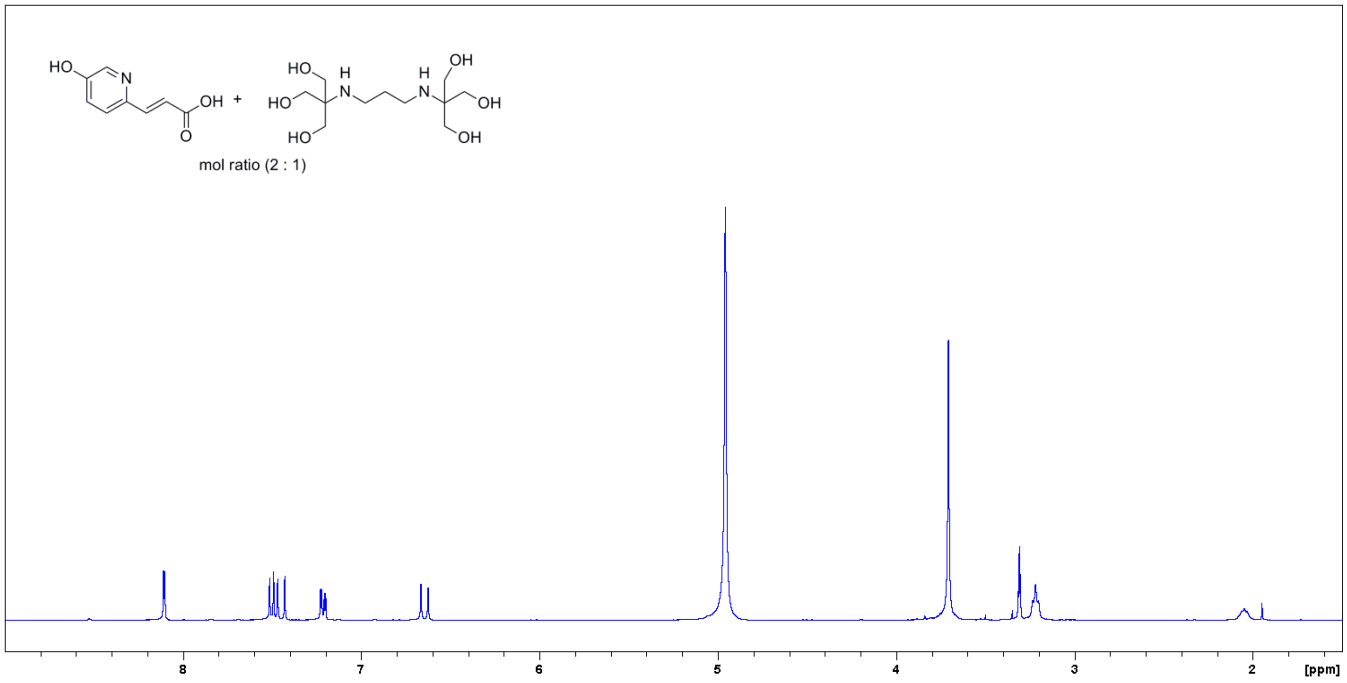

Figure S32. ^{13}C NMR spectrum of enzymatically synthesized 2-aza-4-hydroxycinnamic acid as a BTP complex in D_2O.

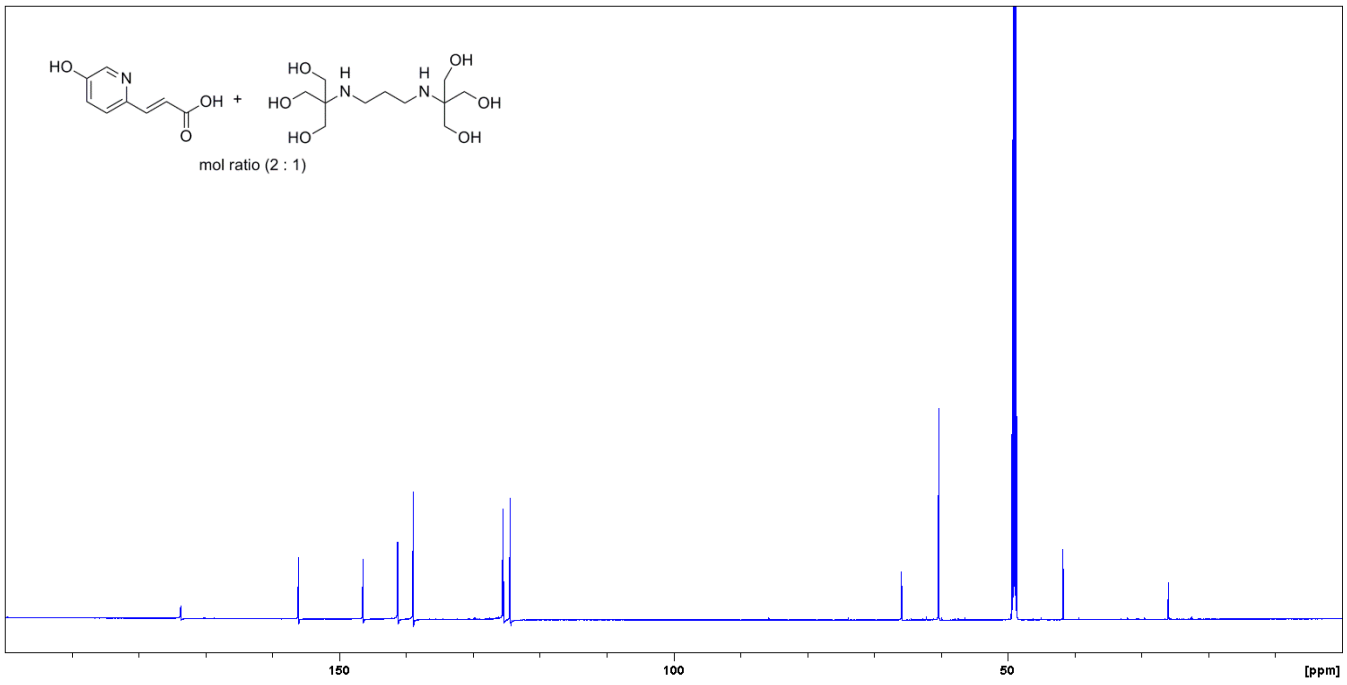

Figure S33. ^{1}H NMR spectrum of enzymatically synthesized (*R*)-2-aza-β-tyrosine methyl ester in CD_3OD.

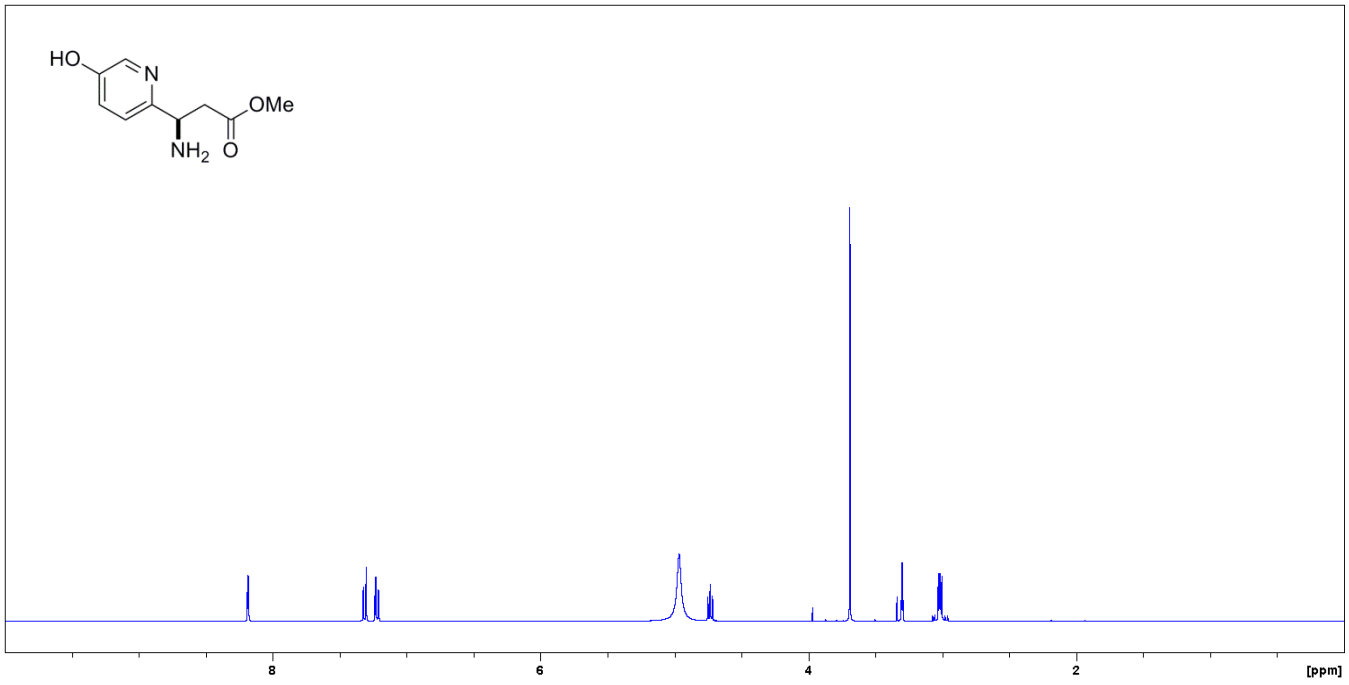

Figure S34. ^{13}C NMR spectrum of enzymatically synthesized (*R*)-2-aza-β-tyrosine methyl ester in CD_3OD.

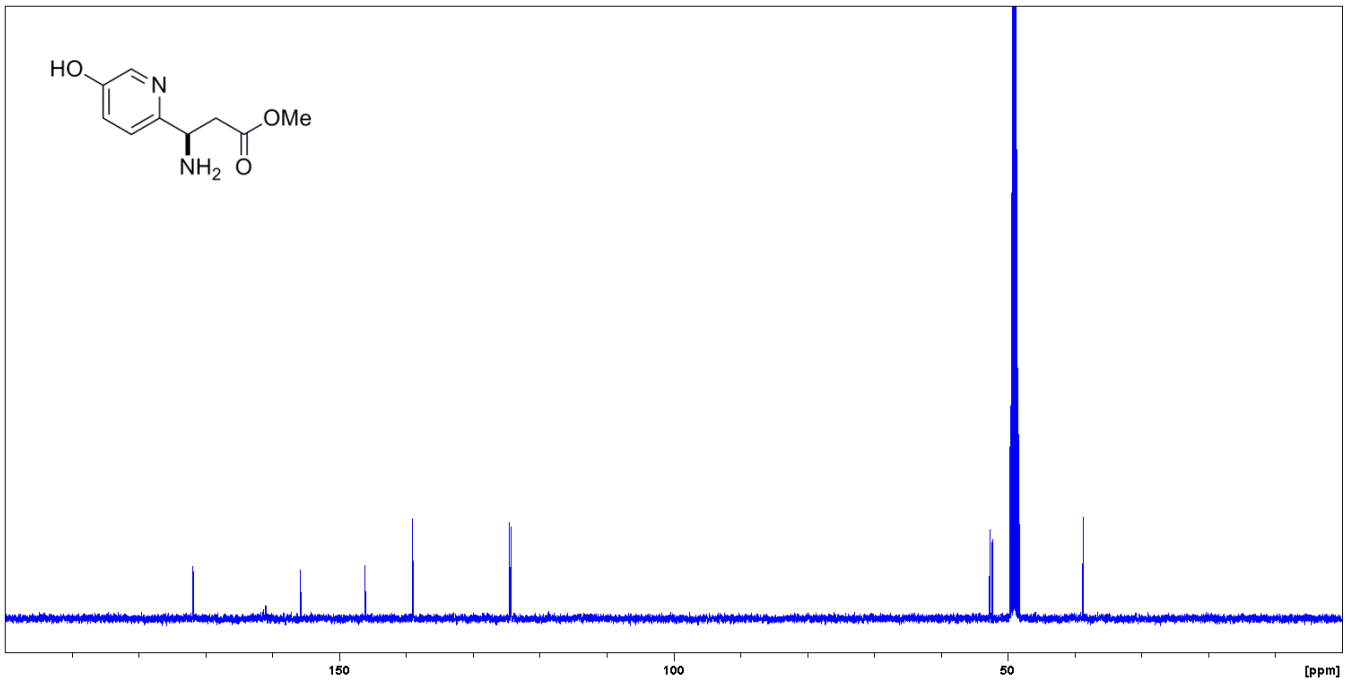

Figure S35. ^{1}H NMR spectrum of (*S*)-MTPA of enzymatically synthesized (*R*)-2-aza-β-tyrosine methyl ester in $CDCl_3$.

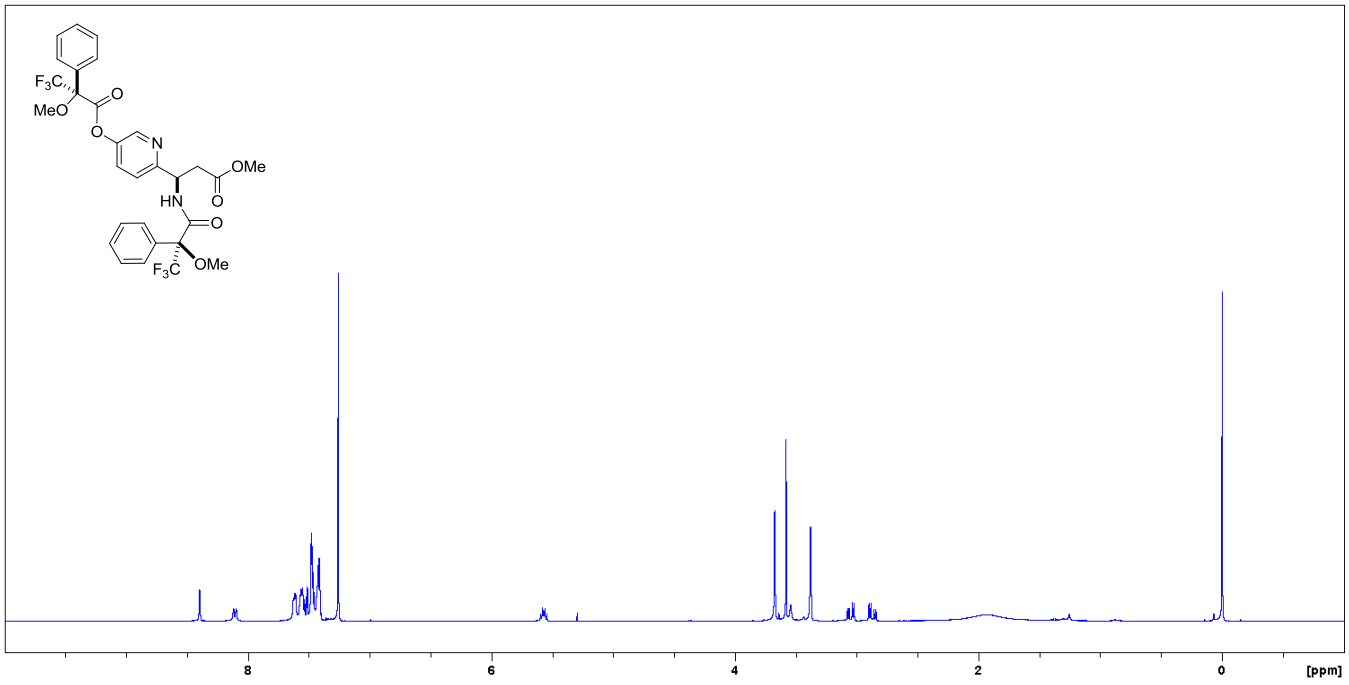

Figure S36. ^{13}C NMR spectrum of (*S*)-MTPA of enzymatically synthesized (*R*)-2-aza-β-tyrosine methyl ester in $CDCl_3$.

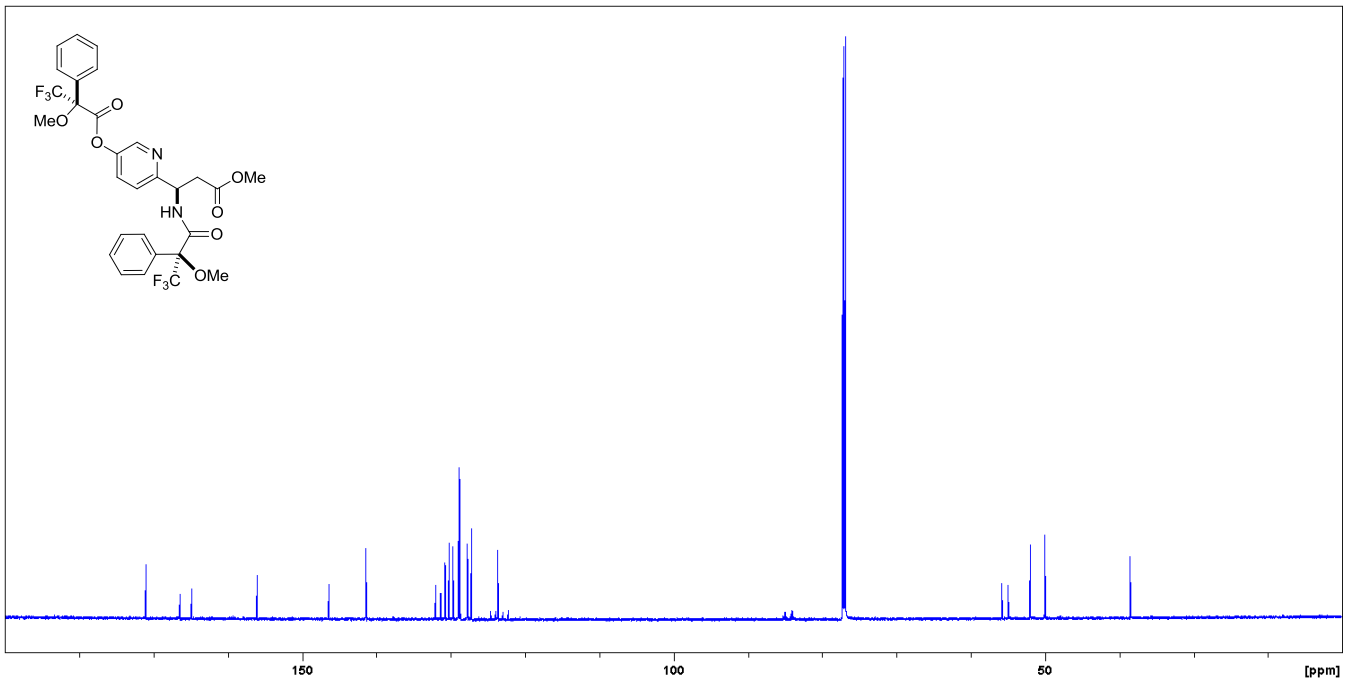

Figure S37. ^{1}H-^{1}H COSY NMR spectrum of (*S*)-MTPA of enzymatically synthesized (*R*)-2-aza-β-tyrosine methyl ester in $CDCl_3$.

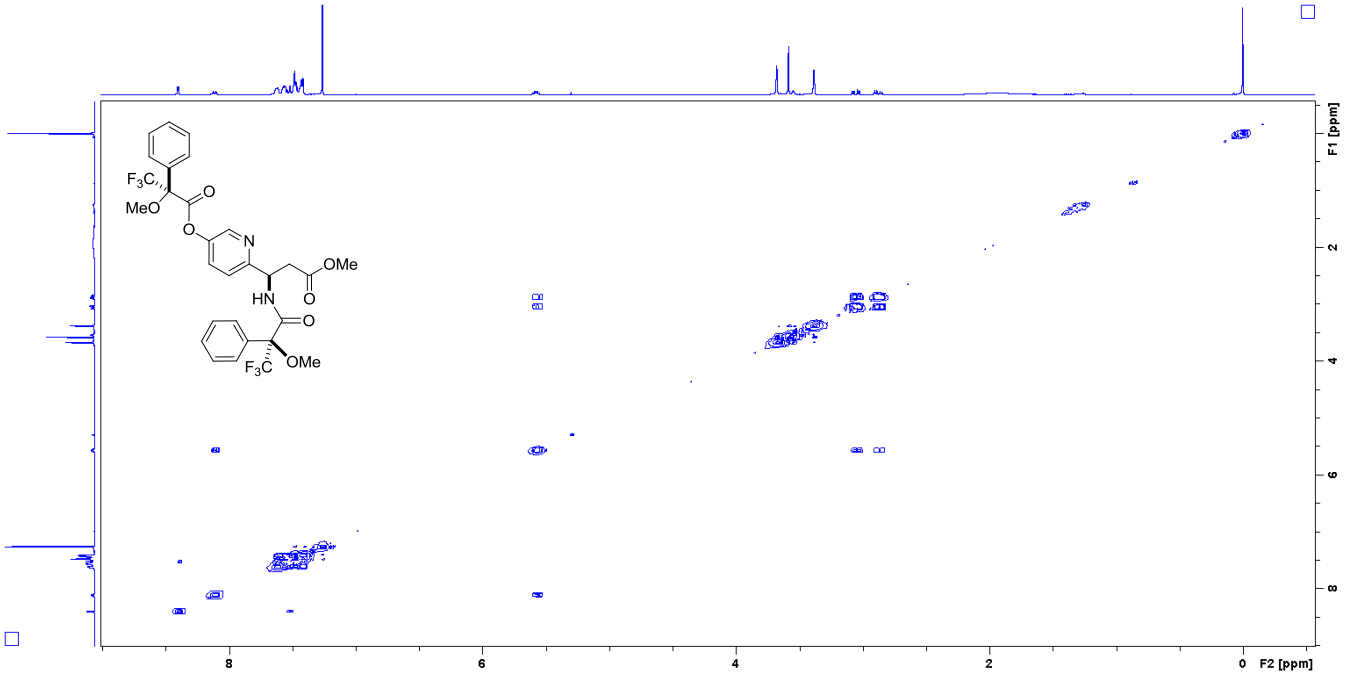

Figure S38. HMBC NMR spectrum of (*S*)-MTPA of enzymatically synthesized (*R*)-2-aza-β-tyrosine methyl ester in $CDCl_3$.

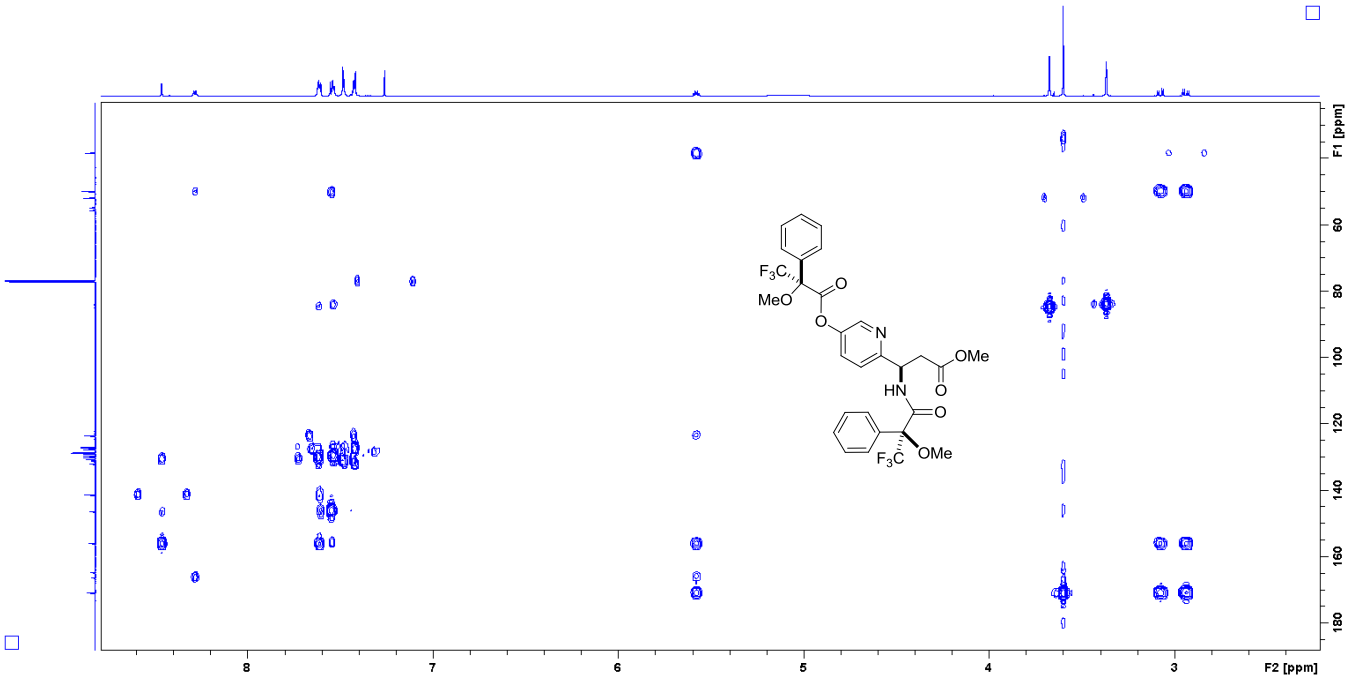

Figure S39. ^{1}H NMR spectrum of (*R*)-MTPA of enzymatically synthesized (*R*)-2-aza-β-tyrosine methyl ester in $CDCl_3$.

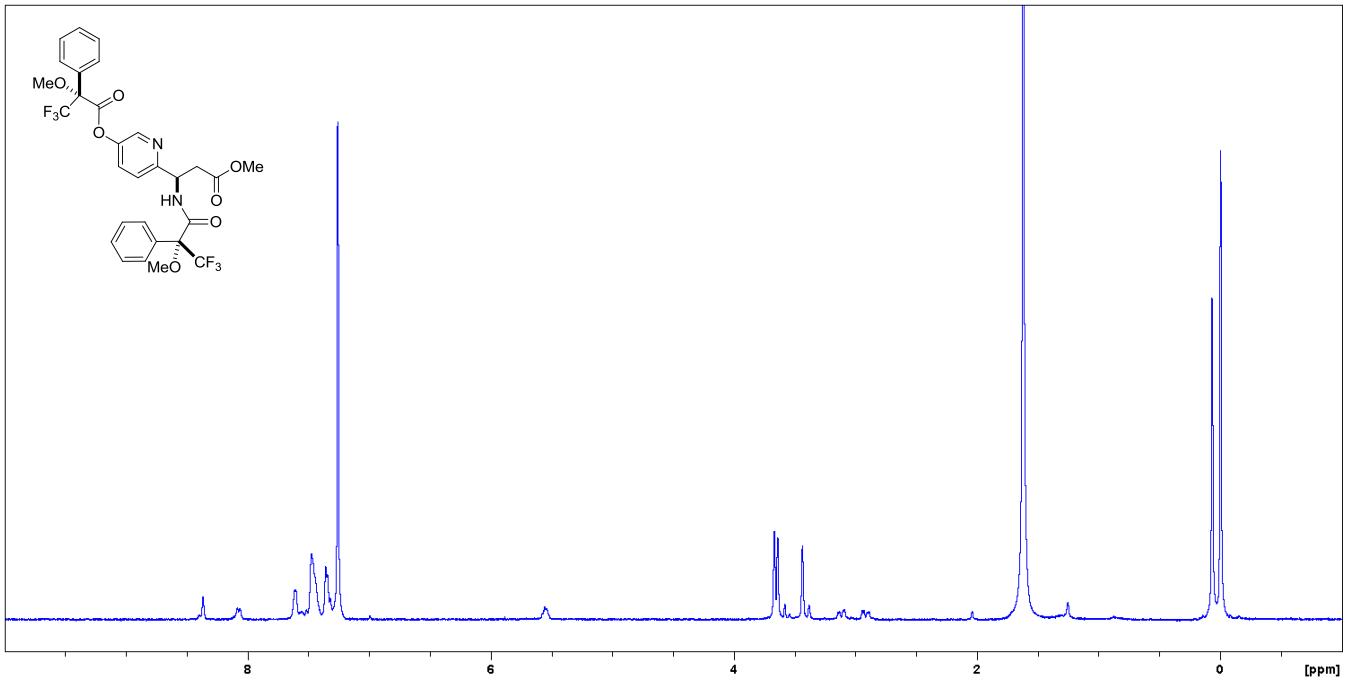

Figure S40. ^{13}C NMR spectrum of (*R*)-MTPA of chemically synthesized (*R*)-2-aza-β-tyrosine methyl ester in $CDCl_3$.

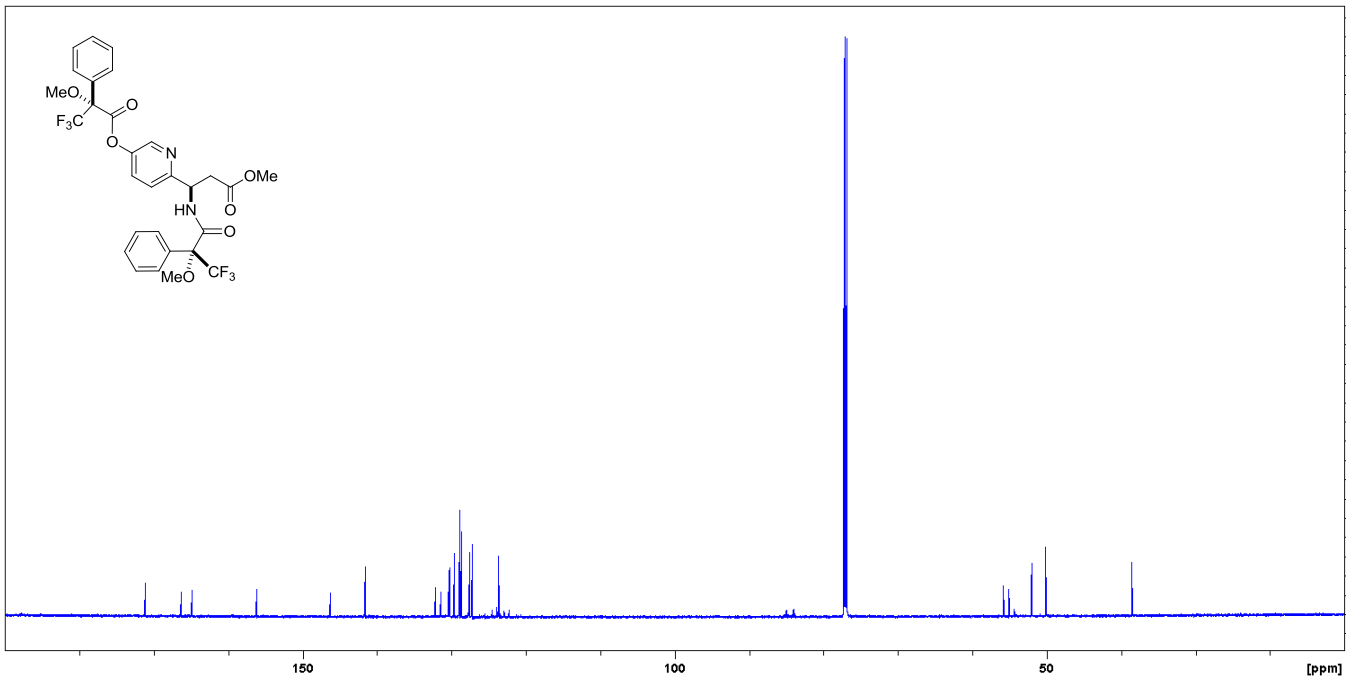

Figure S41. ^{1}H-^{1}H COSY NMR spectrum of (*R*)-MTPA of enzymatically synthesized (*R*)-2-aza-β-tyrosine methyl ester in $CDCl_3$.

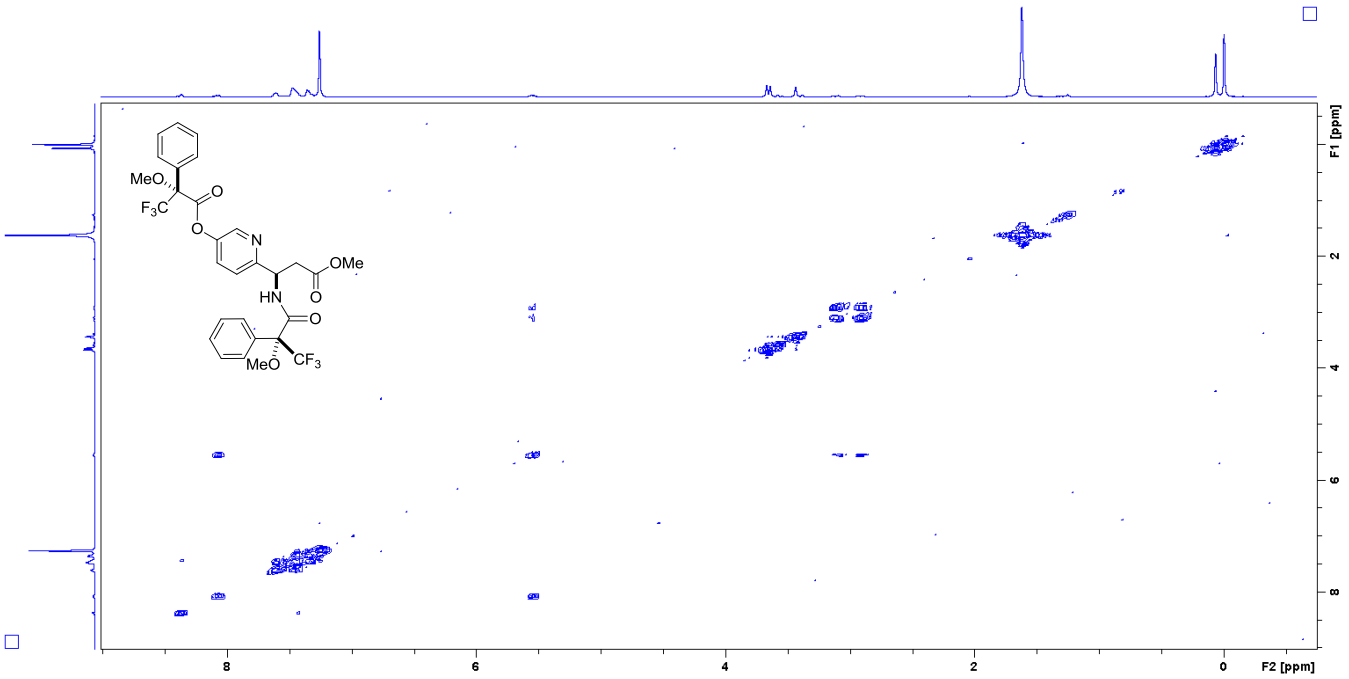

Figure S42. HMBC NMR spectrum of (*R*)-MTPA of chemically synthesized (*R*)-2-aza-β-tyrosine methyl ester in $CDCl_3$.

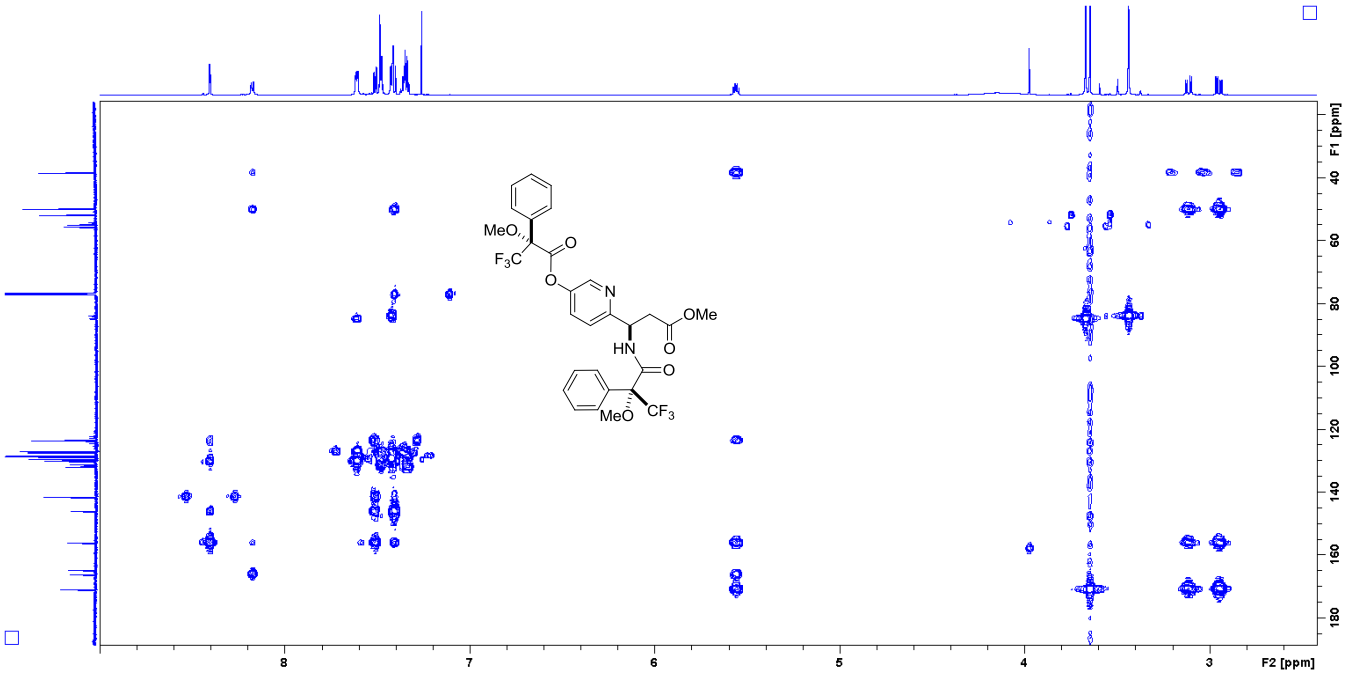

Figure S43. ^{1}H NMR spectrum of (*S*)-MTPA of chemically synthesized (*S*)-2-aza-β-tyrosine methyl ester in $CDCl_3$.

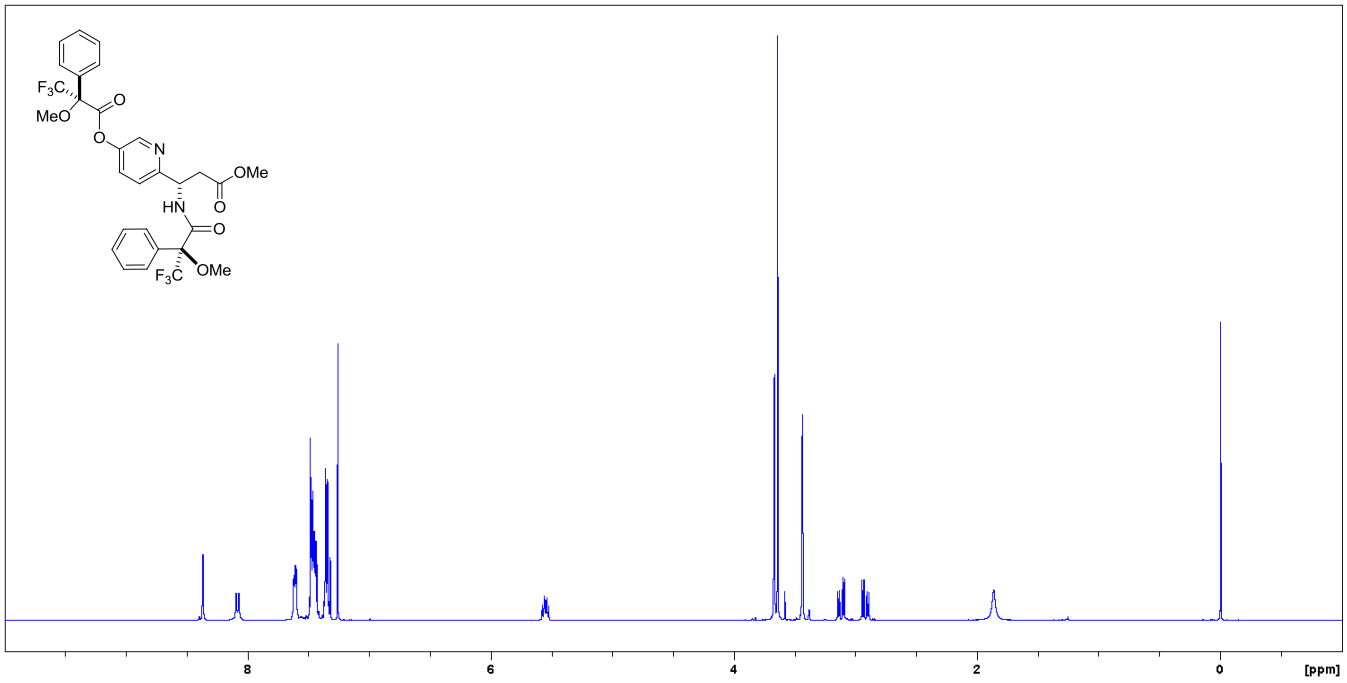

Figure S44. ^{13}C NMR spectrum of (*S*)-MTPA of chemically synthesized (*S*)-2-aza-β-tyrosine methyl ester in $CDCl_3$.

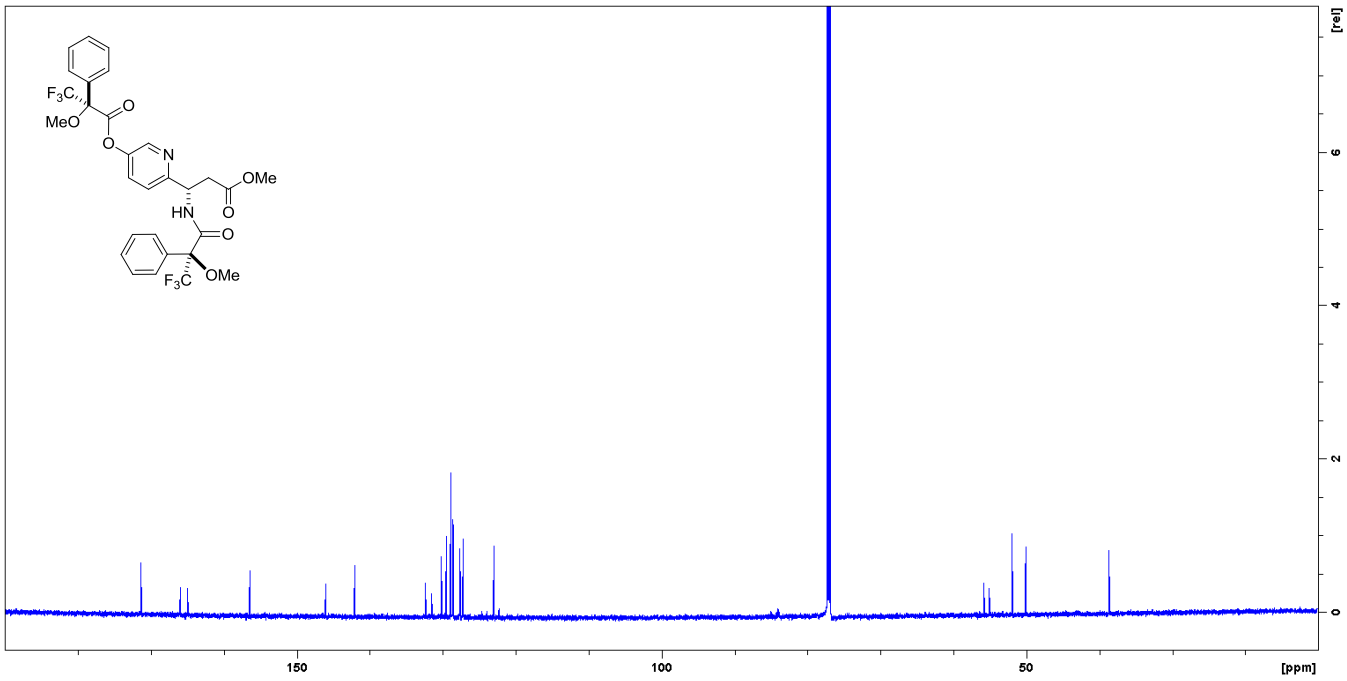

Figure S45. ^{1}H -^{1}H COSY NMR spectrum of (*S*)-MTPA of chemically synthesized (*S*)-2-aza-β-tyrosine methyl ester in $CDCl_3$.

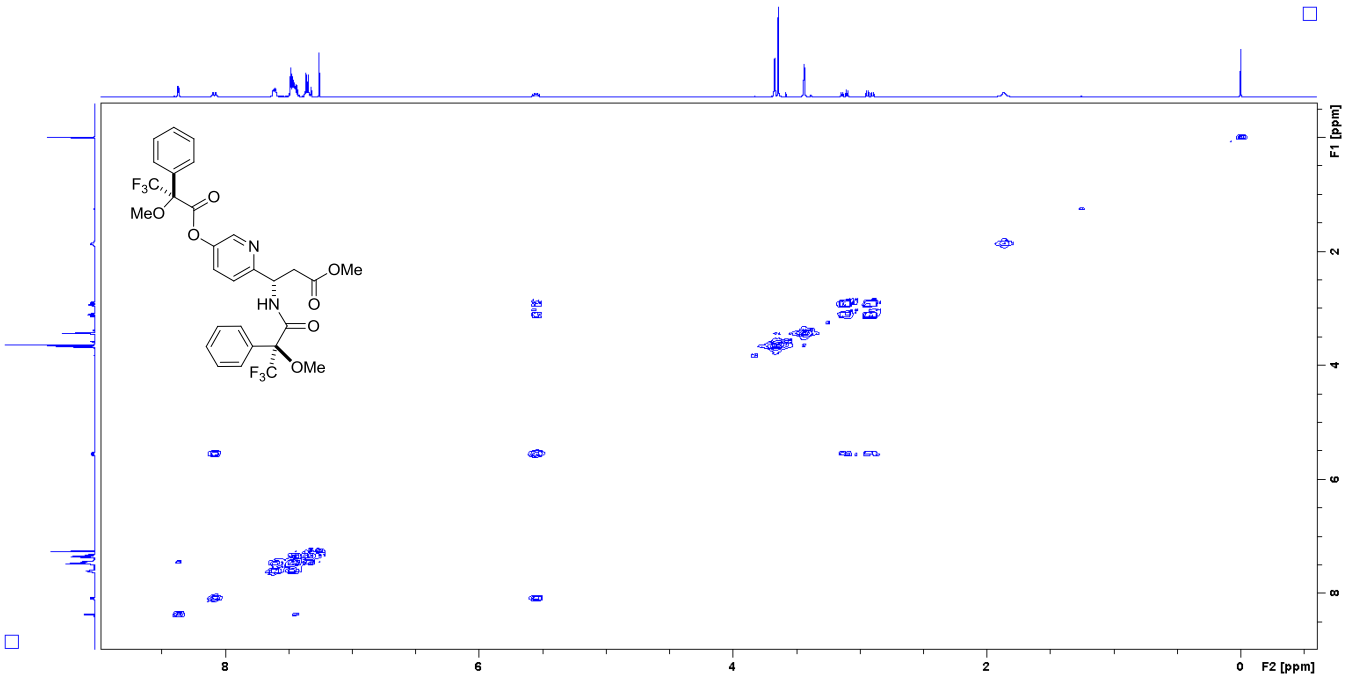

Figure S46. HMBC NMR spectrum of (*S*)-MTPA of chemically synthesized (*S*)-2-aza-β-tyrosine methyl ester in $CDCl_3$.

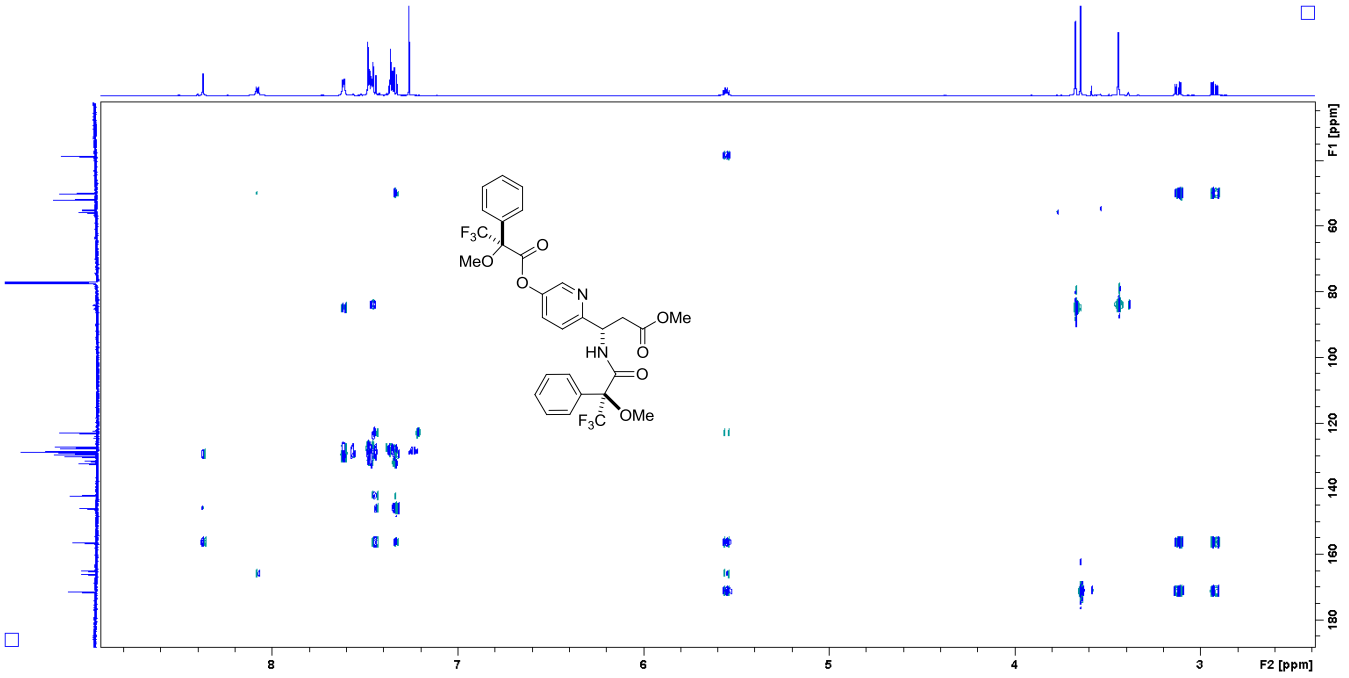

Figure S47. ^{1}H NMR spectrum of (*R*)-MTPA of chemically synthesized (*S*)-2-aza-β-tyrosine methyl ester in $CDCl_3$.

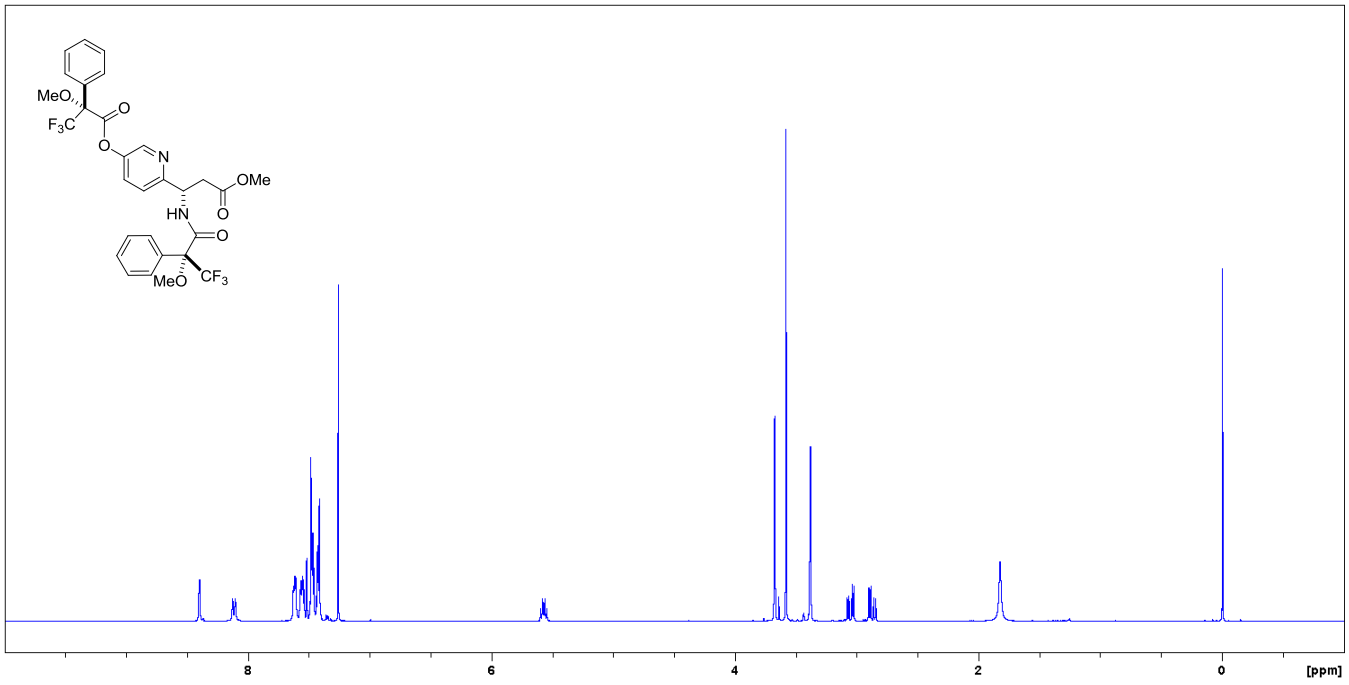

Figure S48. ^{13}C NMR spectrum of (*R*)-MTPA of chemically synthesized (*S*)-2-aza-β-tyrosine methyl ester in $CDCl_3$.

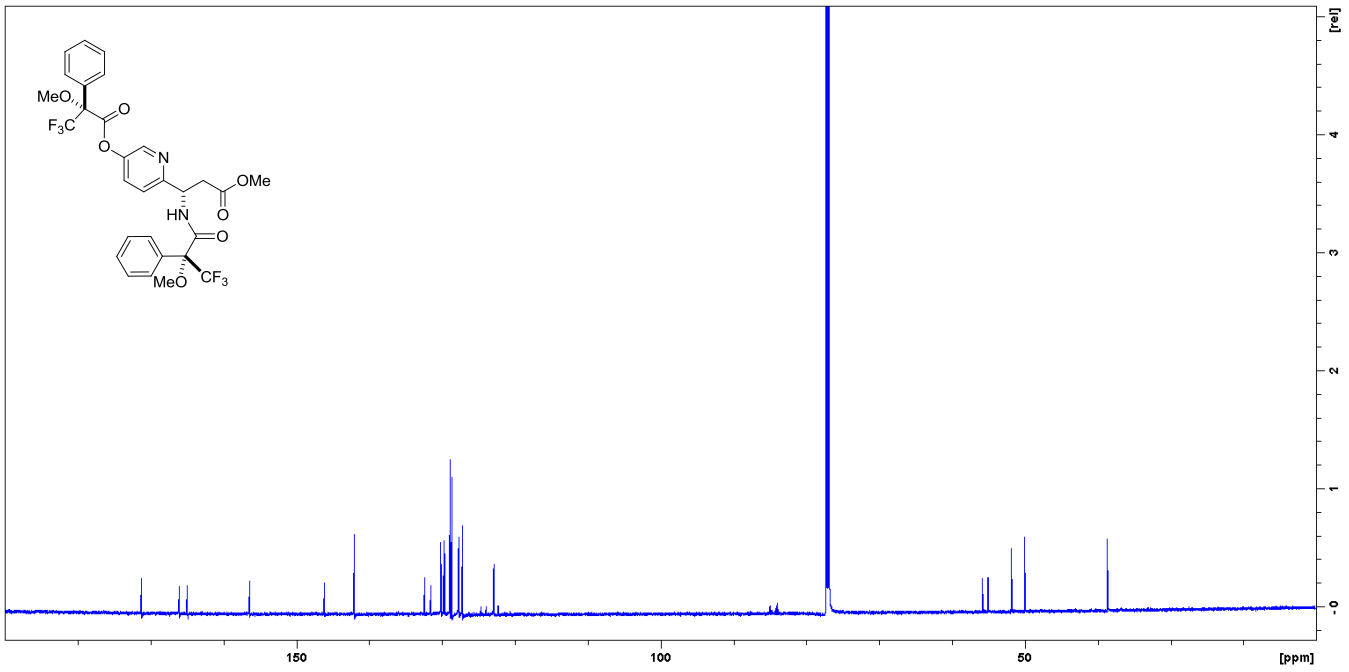

Figure S49. ^{1}H-^{1}H COSY NMR spectrum of (*R*)-MTPA of chemically synthesized (*S*)-2-aza-β-tyrosine methyl ester in in $CDCl_3$.

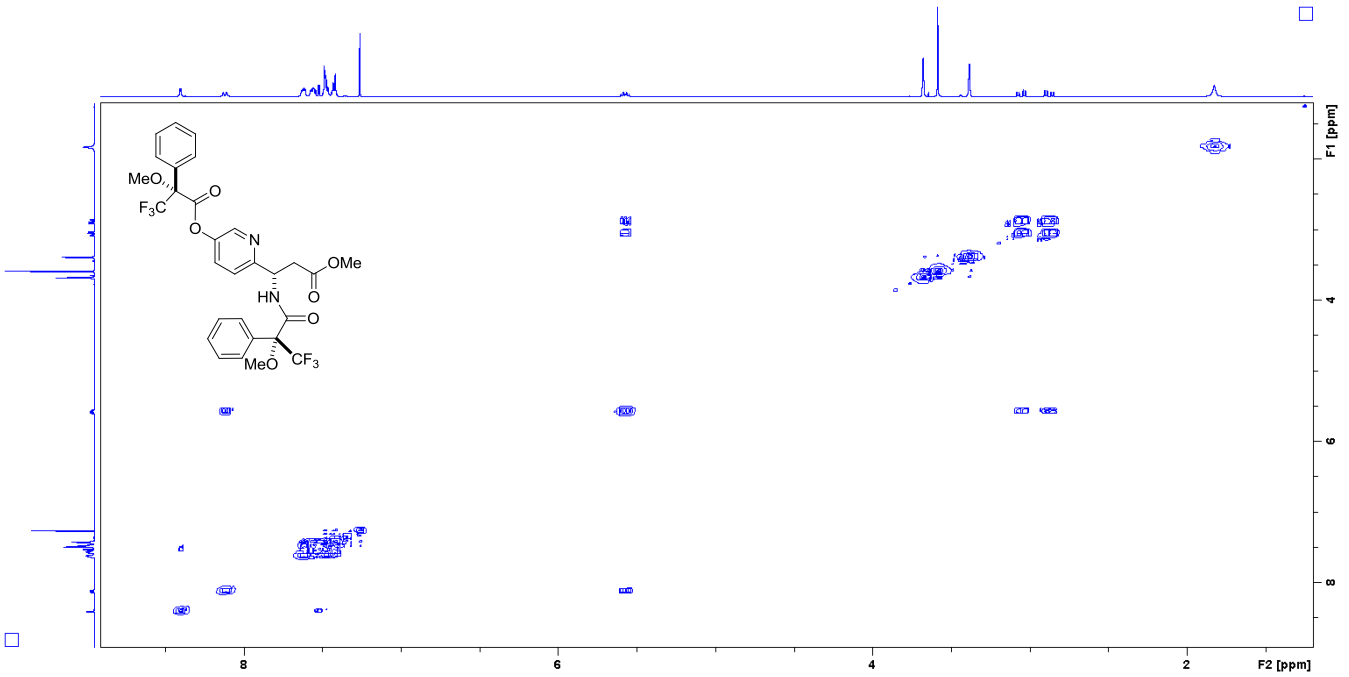

Figure S50. HMBC NMR spectrum of (*R*)-MTPA of chemically synthesized (*S*)-2-aza-β-tyrosine methyl ester in $CDCl_3$.